BMC Cancer

RESEARCH

Open Access

Targeting LLT1 as a potential immunotherapy option for cancer patients non-responsive to existing checkpoint therapies in multiple solid tumors

Tirtha Mandal[1†], Soorya Gnanasegaran[1†], Golding Rodrigues[2†], Shalini Kashipathi[1], Anurag Tiwari[1], Ashvini Kumar Dubey[1], Sanghamitra Bhattacharjee[1], Yogendra Manjunath[1], Subith Krishna[1], M. S. Madhusudhan[2] and Maloy Ghosh[1*]

Abstract

Background High levels of LLT1 expression have been found in several cancers, where it interacts with CD161 on NK cells to facilitate tumor immune escape. Targeting LLT1 could potentially relieve this inhibitory signal and enhance anti-tumor responses mediated through NK cells. Using the 'The Cancer Genome Atlas' (TCGA) database, we investigated the role of LLT1 in the tumor microenvironment (TME) across various cancers. Identifying such biomarkers could create new therapeutic options for patients in addition to complementing existing immunotherapies.

Methods LLT1 expression was evaluated in 33 cancers using TCGA transcriptome data. Univariate Cox regression analysis was employed to assess the correlation of LLT1 expression with patient survival. The relationship between LLT1 expression with immune infiltrates, immune gene signatures, and cancer genomic biomarkers (TMB, MSI, and MMR) was also investigated. Immunofluorescence studies were conducted to validate LLT1 expression in tumors. Furthermore, using the CRI iAtlas data, we evaluated LLT1 distribution and its correlation with other immune checkpoint genes in patients non-responsive to existing immune checkpoint therapies across multiple solid cancers.

Results High expression of LLT1 was observed in 12 cancers, including BRCA, CHOL, ESCA, GBM, HNSC, KIRC, KIRP, LIHC, LUAD, STAD, SARC, and PCPG. In certain cancers like COAD, KICH, and KIRC, high LLT1 expression was associated with poor prognosis. Further analysis revealed that upregulated LLT1 was associated with an abundance of NK and T cell infiltrates in the TME, as well as exhaustive immune biomarkers, and inversely associated with pro-inflammatory and tumor suppressor signatures. High LLT1 expression is also positively correlated with genomic biomarkers in certain cancers. Immunofluorescence studies confirmed moderate to high LLT1 expression in immune-resistant prostate cancer, glioma, ovarian cancer, and immune-sensitive liver cancer cell lines. An independent assessment of clinical cohorts from CRI iAtlas showed a correlation of upregulated LLT1 with multiple immunosuppressive genes in patients non-responsive to current ICIs.

†Tirtha Mandal, Soorya Gnanasegaran and Golding Rodrigues contributed equally to this paper and share first authorship.

*Correspondence:
Maloy Ghosh
maloy.ghosh@zumutor.com
Full list of author information is available at the end of the article

Conclusions The biomarker analysis revealed a clear association between elevated LLT1 expression and an immunosuppressive TME in patient cohorts from TCGA and clinical databases. Therefore, this study provides a foundation for utilizing LLT1 as a potential target to improve clinical responses in ICI non-responsive patients with upregulated LLT1.

Keywords LLT1, Immune Checkpoint Inhibitors, Immunotherapy, Tumor Biomarkers, Tumor Microenvironment, Natural Killer Cells

Background

In recent years, cancer immunotherapy has experienced remarkable advancements, revolutionizing the treatment landscape for various malignancies. Immune checkpoint inhibitors (ICIs) have emerged as a powerful therapeutic approach by unleashing the potential of the immune system to recognize and eradicate cancer cells. While several well-known immune checkpoints have been extensively studied, a growing body of evidence suggests that the LLT1-CD161 axis represents a promising yet relatively unexplored immune checkpoint pathway with immense therapeutic potential [1].

LLT1, also known as CLEC2D (C-type lectin domain family 2 member D), OCIL (Osteoclast inhibitory lectin), and CLAX (Lectin-like NK cell receptor), belongs to the C-type lectin-like receptor superfamily. The human CLEC2D gene has five alternatively spliced variants that result from exon skipping, among which variant 1, or LLT1, was identified as the only protein expressed on the cell surface [2, 3]. As a C-type lectin-like receptor, LLT1 is composed of three domains: a transmembrane domain, a stalk region, and the extracellular carbohydrate recognition domain, which is responsible for receptor recognition. LLT1 is highly glycosylated, and the crystal structure suggests that it homodimerizes at the cell surface, where it serves as a ligand for the NKRP1A (CD161) receptor on NK cells [4]. Among all the previously described isoforms, LLT1 is the only one able to interact with CD161 [2].

Although initially identified in the context of viral infections and auto-immunity, recent studies implicate a role of the LLT1-CD161 axis in modulating immune responses within the tumor microenvironment (TME) of several cancers [5, 6]. LLT1 was reported to be overexpressed in various prostate cancer cell lines (DU145, LNCaP, 22Rv1, and PC3) and primary prostate cancer tissues [7], as well as in glioma cell lines and primary glioblastoma tissues [8]. LLT1 expression was also reported to be upregulated in head and neck squamous cell carcinoma [9], and triple-negative breast cancer [10]. Besides solid tumors, LLT1 overexpression was reported on germinal center-derived B cells in hematological cancers such as non-Hodgkin's lymphoma (NHL) [11]. Interaction of LLT1 with CD161 on NK cells leads to an inhibitory signal that impairs NK cell function, forming an immune evasion mechanism for these cancers. Overall, LLT1 upregulation disrupts cancer immunity through inactivation of NK cells, the first line of immune defense, thereby modulating the TME to become immunosuppressive and favor tumor progression and proliferation.

The TME also hosts several other immunosuppressive cell populations, including regulatory T cells (Tregs) and myeloid-derived suppressor cells (MDSCs). These cell populations are recruited by tumor cells to dampen antitumor immunity in the TME. The secretion of immunomodulatory cytokines by Tregs and MDSCs makes effector immune cells transition into a 'dysfunctional' state, ultimately leading to an immune-resistant TME [12, 13]. Existing ICIs can reprogram the TME through the induction of immune cell activation that changes the cytokine milieu. Despite showing promise in a variety of cancers, ICIs offer benefits to only about 12% of patients across all cancer indications [14]. Therefore, there is a need to identify additional immune checkpoint targets that can potentially benefit patients non-responsive to current immunotherapies.

One such target could emerge from the LLT1-CD161 axis. Therefore, understanding the intricate dynamics of this pathway in the context of cancer could pave the way for the development of novel therapeutic strategies, including augmentation of existing immunotherapeutic approaches. In this work, we focused on elucidating the role of LLT1 in tumor immunity and probed its potential as a biomarker in patients who could benefit from ICIs. By leveraging the TCGA database, we performed an extensive pan-cancer analysis to assess LLT1 differential gene expression profiles, patient survival outcomes, GSEA (CNV, methylation, pathway) analyses, correlations with immune gene signatures, tumor-infiltrating immune cells, and tumor genomic markers (tumor mutational burden: TMB and microsatellite instability: MSI). Expression of LLT1 on various tumors was experimentally assessed using an anti-LLT1 monoclonal antibody. In addition, we utilized a clinical dataset from the CRI iAtlas portal to assess LLT1's potential as a biomarker in patients non-responsive to current ICIs.

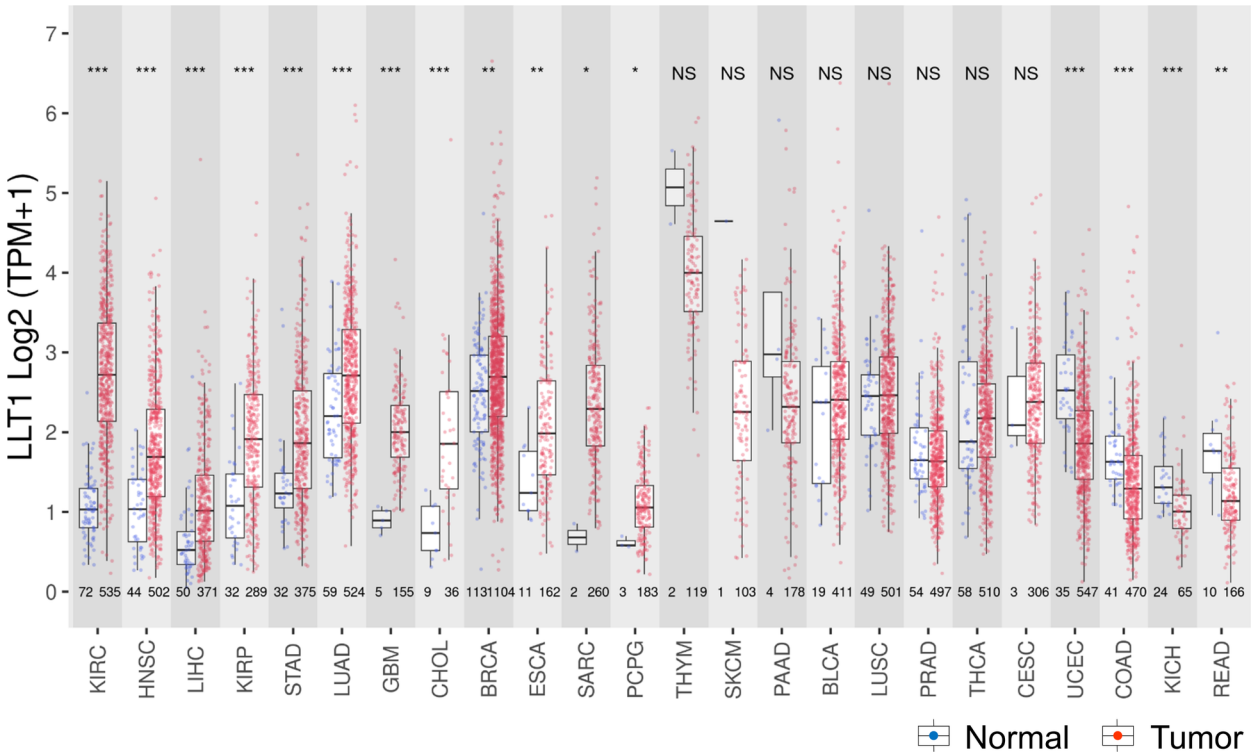

Fig. 1 LLT1 expression across tumors and normal adjacent tissues. **A** LLT1 expression in the indicated cancer types. The Mann-Whitney test was used to compare the difference in LLT1 expression between the tumor and its adjacent normal. Cancers that have significantly higher LLT1 expression in the tumor tissue compared to the normal are shown on the left. **B** Cancer types that did not contain data for adjacent normal tissue in the GDC database accessed through the UCSC Xena browser. **C** The expression levels of LLT1 transcripts across different AJCC pathologic stages compared to the adjacent normal expression levels through the Mann-Whitney Test. LLT1 expression tends to be higher in higher stages compared to normals. *$P < 0.05$, ** $P < 0.01$, *** $P < 0.001$. **D** Plot showing the correlation between the expression of LLT1 and methylation across different cancer types. The size of the dots represents the adjusted p-values, and the color represents the correlation coefficient. Unfaded dots represent statistically significant data points, while the faded dots represent statistically insignificant data points. **E** CNV profile showing percentage of heterozygous or homozygous CNV, including amplification or deletion for the LLT1 gene in each cancer. **F** Plot showing the correlation between the expression of LLT1 and CNV across different cancer types. The size of the dots represents the adjusted p-values, and the color represents the correlation coefficient. Unfaded dots represent statistically significant data points, while the faded dots represent statistically insignificant data points

Results

LLT1 expression profiles in human cancers

The comparison of pan-cancer LLT1 expression profiles between tumor and adjacent normal samples was evaluated from the TCGA dataset (Fig. 1A). Along with this, a tumor-only dataset lacking adjacent normal samples was also analyzed (Fig. 1B). The adjacent normal samples refer to histologically normal tissue adjacent to the tumor. The LLT1 expression profiles were segregated into cancers with significantly high (left) to significantly low LLT1 expression (right), with non-significant cancers shown in between (Fig. 1A). High LLT1 expression ($p < 0.05$) was observed in 12 tumor types: BRCA, CHOL, ESCA, GBM, HNSC, KIRC, KIRP, LIHC, LUAD, STAD, SARC, and PCPG, compared to their adjacent normals (Fig. 1A). Notably, in LIHC, BRCA, HNSC, and LUAD, an elevated expression was observed compared to normal across nearly all cancer stages (Fig. 1C; Table 1). Among these, HNSC had stage-wise subpopulations that were the most significantly different ($p < 0.001$). Among all 33 cancers, this subset of cancers showed significantly increased stage-wise expression of LLT1. In addition, from the tumor-only dataset, it's evident that DLBC and LAML had the highest absolute median expression value among all tumor types (Fig. 1B).

To validate these findings, an independent database, CCLE [15], was used to obtain LLT1 expression profiles from cell lines corresponding to 24 different tissues. Interestingly, we observed similar expression patterns – out of 12 tumors in TCGA that showed LLT1 upregulation, 10 of them showed the same pattern in CCLE

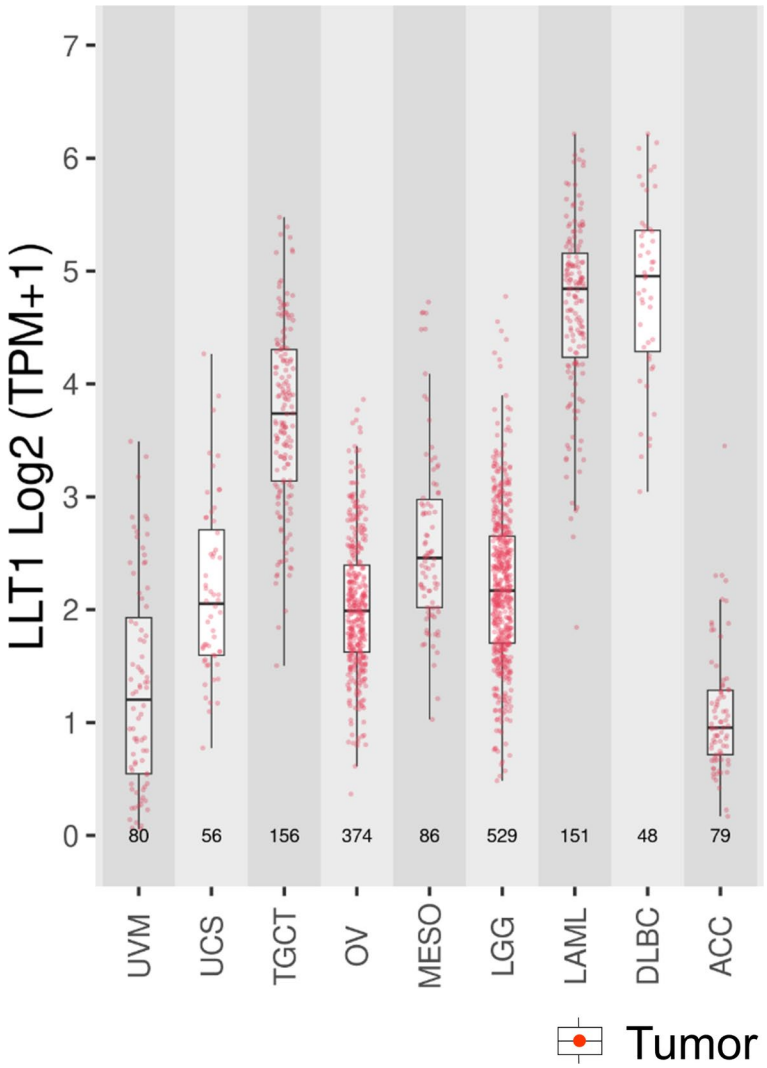

Fig. 1 continued

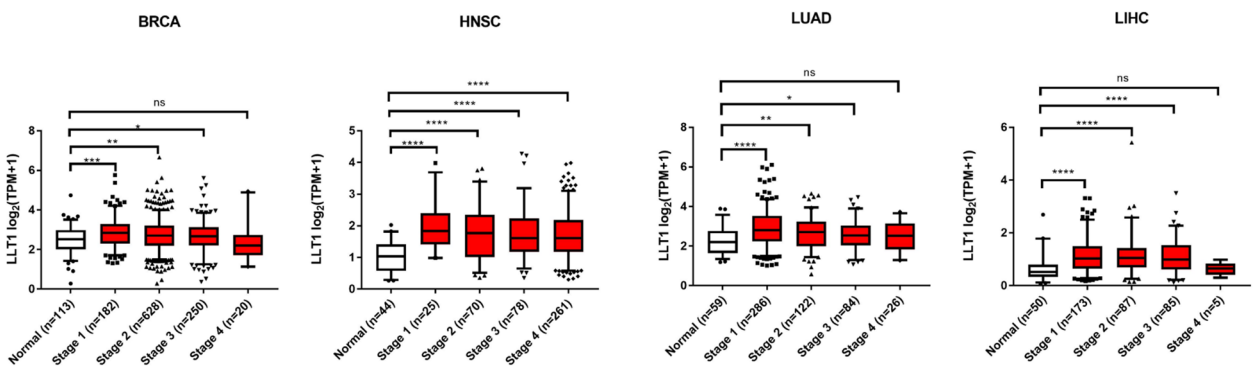

Fig. 1 continued

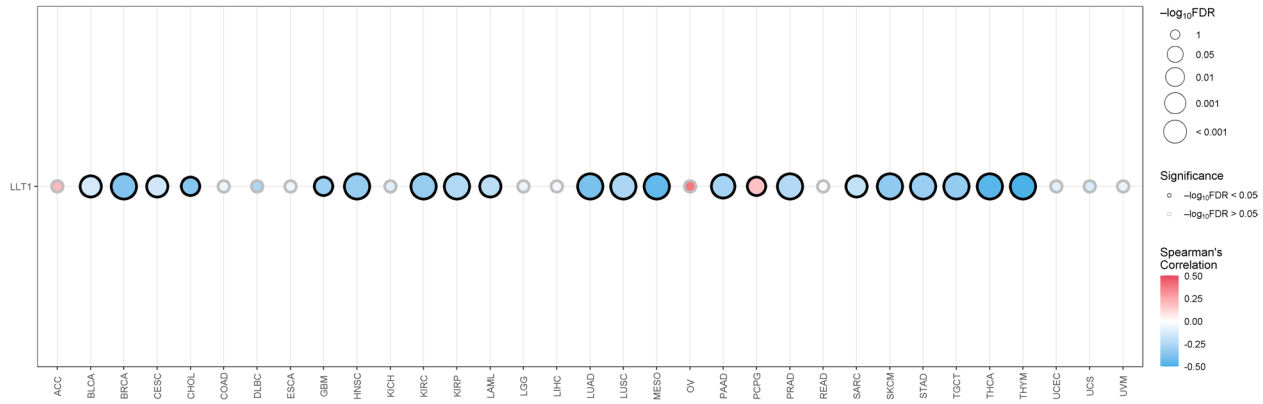

Fig. 1 continued

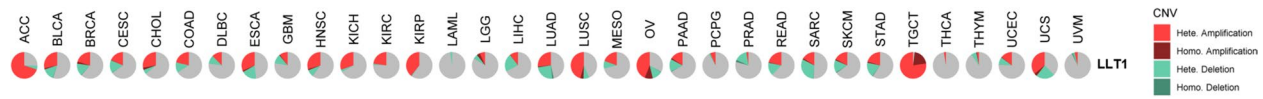

Fig. 1 continued

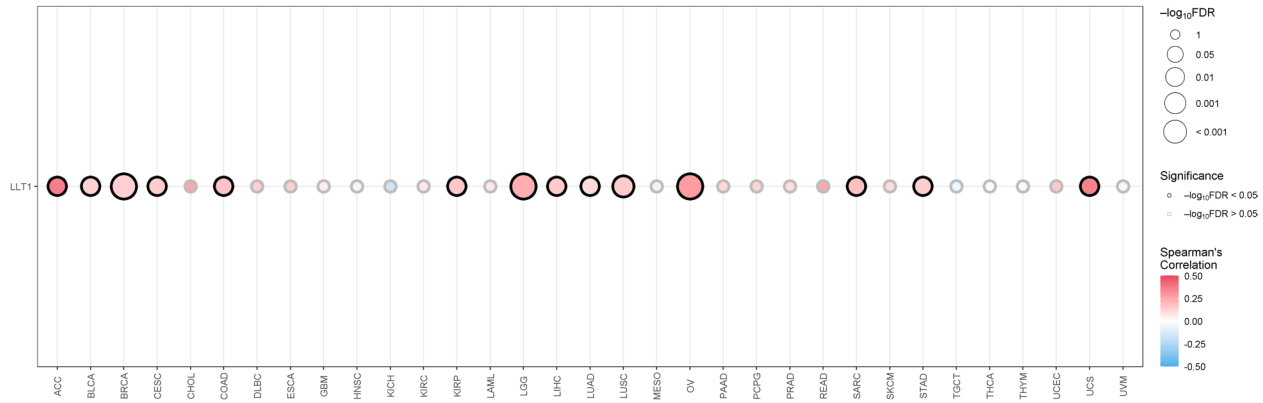

Fig. 1 continued

Table 1 TPM values for normal and cancer tissues

	Adjacent Normal	Stage 1	Stage 2	Stage 3	Stage 4
BRCA	2.516 (2.005–2.967)	2.851 (2.307–3.285)	2.705 (2.19–3.216)	2.669 (2.211–3.135)	2.196 (1.804–2.709)
HNSC	1.034 (0.626–1.409)	1.837 (1.445–2.324)	1.768 (1.023–2.341)	1.608 (1.181–2.221)	1.608 (1.18–2.181)
LIHC	0.523 (0.342–0.753)	1.027 (0.651–1.475)	1.052 (0.709–1.422)	0.995 (0.62–1.529)	0.649 (0.529–0.687)
LUAD	2.201 (1.679–2.736)	2.811 (2.239–3.526)	2.711 (2.012–3.208)	2.535 (2.036–3.021)	2.531 (1.915–3.115)

(Fig. S1, Table S1). Statistically, the expression trends seen in the TCGA dataset were similar to those observed in the CCLE dataset.

Pan-cancer methylation analysis of LLT1

We explored the epigenetic regulation of LLT1 expression through DNA methylation analysis. Using the GSCA

platform, we evaluated the methylation status of LLT1 across 33 cancers from TCGA. The results indicated that LLT1 expression was negatively correlated (Spearman's rho < -0.2) with methylation levels across a large subset of cancers like BRCA, CHOL, GBM, HNSC, KIRC, KIRP, LUAD, STAD, and SARC (Fig. 1D). The correlations were also statistically significant. Interestingly, in these cancers, an upregulated LLT1 expression was also observed, suggesting a link between methylation status and LLT1 gene expression in human cancers.

Furthermore, DNA methylation can be a valuable tool for classifying meningiomas [16]. Tumors can be categorized based on their unique methylation patterns and defined by specific biological characteristics such as DNA mutations, RNA levels, and protein levels. There are four tumor groups: the immunogenic group marked by an influx of immune cells, the benign NF2-wildtype group characterized by at least one normal copy of the NF2 gene, the hypermetabolic group with increased activity of genes regulating cell metabolism, and the proliferative group characterized by genetic and epigenetic changes leading to continuous cell division. Our analysis revealed variations in LLT1 expression among these subtypes. Notably, the immunogenic subtype exhibited the highest levels of LLT1 expression, which differed significantly from the other subtypes (Fig. S2). The expression of LLT1 appears to be linked to the differences in methylation patterns observed in meningioma.

Pan-cancer analysis of copy number variation (CNV) distribution in LLT1

We performed the copy number variation (CNV) analysis using the GSCA platform. We found different types of CNV of the target LLT1 gene, with major types being heterozygous amplification or deletion and minor types being homozygous amplification or deletion. The results showed that in ACC, BLCA, BRCA, COAD, CHOL, ESCA, HNSC, KICH, KIRC, KIRP, LUSC, SKCM, STAD, OV, TGCT, and UCS, the fraction of heterozygous amplifications was higher compared to other CNVs (Fig. 1E). The amount of copy number amplification occupied 15–20% of the total variant copy number count on average for the tumors. In the correlation analysis, a subset of cancers including BLCA, BRCA, KIRP, LGG, LIHC, LUAD, SARC, STAD, and OV exhibit significant positive correlation (Spearman's rho > 0.15) with LLT1 expression (Fig. 1F). This pan-cancer analysis revealed that heterozygous amplification or deletion was the most commonly observed CNVs and showed an association between CNV and LLT1 expression.

Association of LLT1 expression and patient survival

We next investigated the relationship between LLT1 expression and patient survival in 33 cancers. The Cox regression analysis showed that high LLT1 expression was associated with poor prognosis in KICH (HR: 2.114, 95% CI: 1.265–3.534), COAD (HR: 1.114, 95% CI: 1.004–1.237), and KIRC (HR: 1.067, 95% CI: 1.038–1.096) (Fig. 2A; Table 2). Despite low LLT1 expression levels being observed in COAD and KICH (Fig. 1A), they still affected survival in these cancers (Fig. 2B). In KIRC though, a consistent pattern was observed where high LLT1 expression correlated with poor survival, evident from the Kaplan-Meier curves (Fig. 2B). Also, the survival analysis of these specific cancers from an independent database, PRECOG, showed similar outcomes. In 2 out of 4 COAD datasets (GSE12945 and GSE16125), even though a difference in survival probabilities was observed, elevated LLT1 expression was associated with poor prognosis (Fig. S3). In KICH [17], the same survival pattern was observed as well (Fig. S3). Interestingly, in a subset of cancers like BRCA, LUAD, HNSC, BLCA, and CESC, the hazard ratio is significant ($p < 0.05$) and less than 1, suggesting LLT1 is associated with a favorable prognosis in these cancer types (Fig. 2A; Table 2). The expression of LLT1 in both immune cells and tumor cells in the TME, as observed in multiple studies with LUAD and HNSC [6, 18], suggests that LLT1 can have variable effects on prognosis depending on the tumor type. Hence, further analysis of LLT1 expression on tumor cells and its correlation with disease outcome needs to be carried out to understand the role of LLT1 in TME of certain specific cancers.

Gene set enrichment analysis (GSEA) of LLT1 using HALLMARK terms

To examine LLT1's role in innate and adaptive immunity and cancer, we used the HALLMARK pathways database to identify the functional pathways associated with LLT1 across the TME of 33 cancers. Across nearly all the cancer types, several immune-related pathways like IL2-STAT5 signaling, IL6-JAK-STAT3 signaling, inflammatory response, allograft rejection, and oncogenic pathways like KRAS signaling, PI3K-AKT-MTOR signaling, and epithelial-mesenchymal transition were positively enriched in the high LLT1 group (Fig. 3). This provides empirical evidence supporting the conception that LLT1 is intricately involved in the immune response pathways and drives oncogenic signaling in the TME.

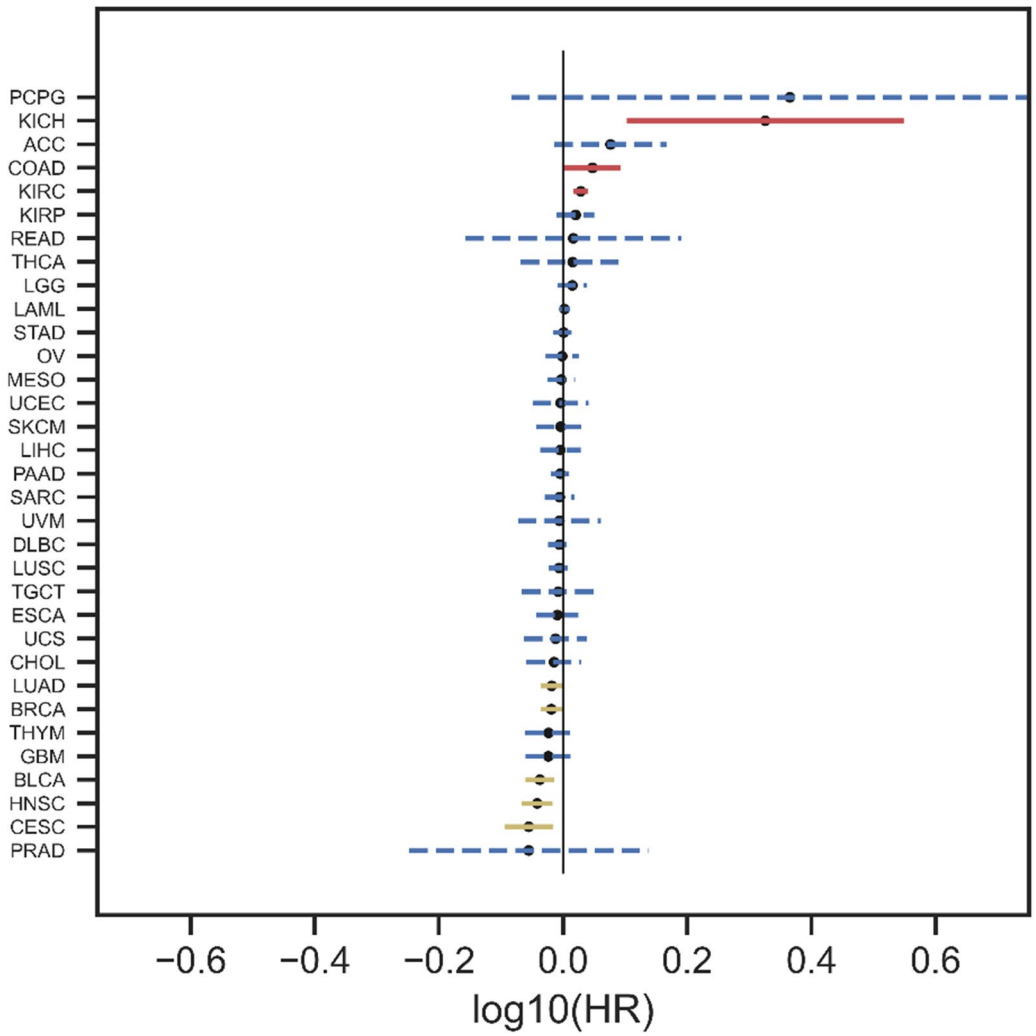

Fig. 2 Association of LLT1 expression with patient prognosis. **A** Univariate Cox-Proportional Hazards regression was performed with LLT1 expression as the independent variable, and overall survival information was obtained through the clinical files associated with each of the cancers. LLT1 was found to be a prognostic risk factor in KIRC, KICH, and COAD with Hazard ratios significantly more than 1. (KIRC-HR = 1.067, KICH-HR = 2.114, and COAD-HR = 1.114) **B** The empirically estimated Kaplan Meier Curves for these three cancers. The 'High' group shown in red is the sub-population of patients whose LLT1 expression is higher than its median as measured in TPM, while the 'Low' group shown in blue is the population of patients who have LLT1 expression lower than its median as measured in TPM

Immune cell infiltration in TME is correlated with LLT1 expression

We next examined whether LLT1 affects the abundance of immune infiltrates that have prognostic value in the TME. To do this, we explored the relationship between LLT1 expression and immune cell infiltration in 33 tumor types using an immune infiltration analysis tool called CIBERSORT. To establish a regulatory role of LLT1 in the TME, we examined the association between immune cell infiltration scores estimated from the bulk transcriptomic data in TCGA and correlated it with LLT1 expression. In LIHC, LUAD, PAAD, KIRC, PRAD, LUSC, SKCM, THCA, BRCA, KIRP, STAD, ESCA, and THYM, the expression of LLT1 was positively (Spearman's rho > 0.3) associated with the infiltration of CD8 + T cells, CD4 + T cells (memory activated), and activated NK cells (Fig. 4). On the other hand, in LIHC, PAAD, CHOL, and THYM, the expression of LLT1 was positively associated (Spearman's rho > 0.3) with the infiltration of immunosuppressive Tregs while showing a negative association with the infiltration of CD4 + Naïve T cells in THCA and KICH (Fig. 4). There was an association of LLT1 expression with activated effector immune cell infiltrates, with additional implications of tolerant Treg cells being present in the TME of certain cancers. The association of

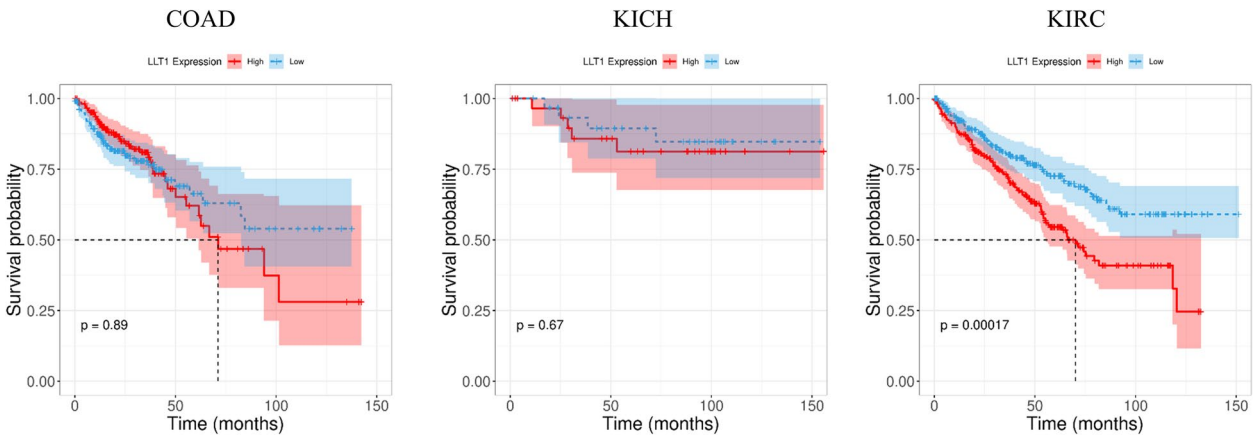

Fig. 2 continued

Table 2 Cox regression analysis of LLT1 in 33 cancers

Cancers	HR (± 95% CI)	*P*-value
PCPG	2.316 (0.825–6.504)	0.1106
KICH	2.114 (1.265–3.534)	0.0042
ACC	1.190 (0.967–1.465)	0.0994
COAD	1.114 (1.004–1.237)	0.0405
KIRC	1.067 (1.038–1.096)	2.41E-06
KIRP	1.046 (0.976–1.121)	0.2012
READ	1.037 (0.695–1.547)	0.8553
THCA	1.035 (0.853–1.255)	0.7240
LGG	1.033 (0.978–1.092)	0.2356
LAML	1.004 (0.985–1.023)	0.6216
STAD	1.000 (0.963–1.040)	0.9605
OV	0.995 (0.936–1.059)	0.8903
MESO	0.992 (0.942–1.045)	0.7721
UCEC	0.990 (0.893–1.098)	0.8581
SKCM	0.990 (0.903–1.085)	0.8381
LIHC	0.989 (0.918–1.066)	0.7843
PAAD	0.988 (0.954–1.024)	0.5315
SARC	0.986 (0.933–1.043)	0.6409
UVM	0.985 (0.855–1.1498)	0.8410
DLBC	0.985 (0.945–1.028)	0.4960
LUSC	0.984(0.947–1.022)	0.4129
TGCT	0.981(0.857–1.123)	0.7896
ESCA	0.977(0.904–1.057)	0.5730
UCS	0.971(0.864–1.091)	0.6278
CHOL	0.966(0.872–1.069)	0.5067
LUAD	0.957(0.920–0.996)	0.0331
BRCA	0.956(0.918–0.996)	0.0316
THYM	0.947(0.868–1.033)	0.2198
GBM	0.946(0.868–1.031)	0.2041
BLCA	0.916(0.869–0.967)	0.0013
HNSC	0.907(0.857–0.961)	0.0008
CESC	0.880(0.804–0.963)	0.0055
PRAD	0.879(0.564–1.370)	0.5710

LLT1 expression with poor prognosis in KIRC may be explained by the presence of both effector and tolerant immune cell infiltrates in the TME (Fig. 2B). Similarly, the presence of immunosuppressive Tregs in multiple other cancers can dampen the pro-tumor immune response despite the presence of effector T and NK immune cell infiltrates in the TME.

Correlation of immune checkpoint genes with LLT1 expression

To further correlate the elevated LLT1 expression with an immunosuppressive phenotype, we computed the correlation values to several important immune checkpoint genes. We observed that LLT1 is positively correlated (Pearson's $R > 0.3$, $p < 0.05$) to immunosuppressive genes such as *TIGIT*, *LAG3*, *CD274 (PD-L1)*, *HAVCR2 (TIM-3)*, *IL4*, *IL10*, *IDO1*, *ARG1*, *ICOS*, *CD39*, *CCL17*, *FOXP3*, and *CD33* in nearly all 33 cancer types (Fig. 5A). In line with these observations, LLT1 was negatively correlated (Pearson's $R < -0.2$, $p < 0.05$) to a few pro-inflammatory and several tumor suppressor genes such as *LAMP1 (CD107a)*, *IL-1B*, *A2M*, *PTEN*, *HLA-E*, *ULBP1*, *LKB-1*, *BAD*, and *SLAMF9* (Fig. 5A). For specific cancers, the individual correlation plots for some key immunosuppressive and immune-inflammatory/ tumor repressor genes are shown (Fig. 5B). Also, the GSEA analysis of LLT1 based on the immunosuppressive genes shows enrichment of pathways related to T cell tolerance, inflammation, and myeloid cell regulation (Fig. 5C). These results collectively suggest that despite there being evidence of association of LLT1 expression with prior immune activation, this succumbs to the immune suppressive mechanisms present in the TME. Such mechanisms likely affect tumor progression, which could ultimately influence patient survival.

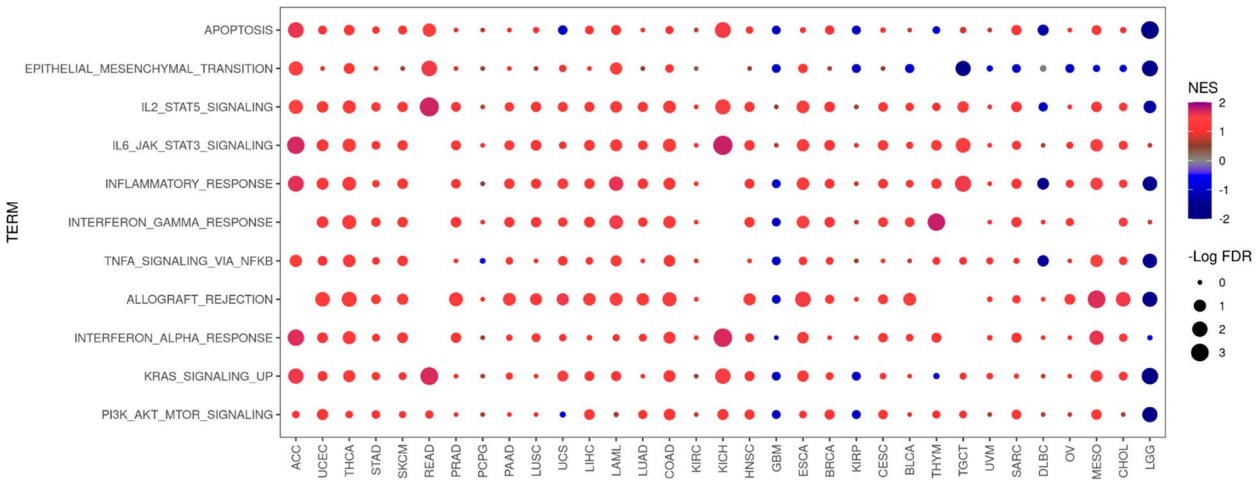

Fig. 3 LLT1-related gene set enrichment analysis. The Normalized Enrichment Score (NES) for important cancer-relevant pathways from the Hallmark Pathways gene sets was estimated across 33 cancers. Positive NES indicates an enrichment of that pathway in the 'High LLT1 expression' group while a negative NES score indicates an enrichment of that pathway in the 'Low LLT1 expression' group in a given cancer. The sizes of the dots are indicative of the level of enrichment

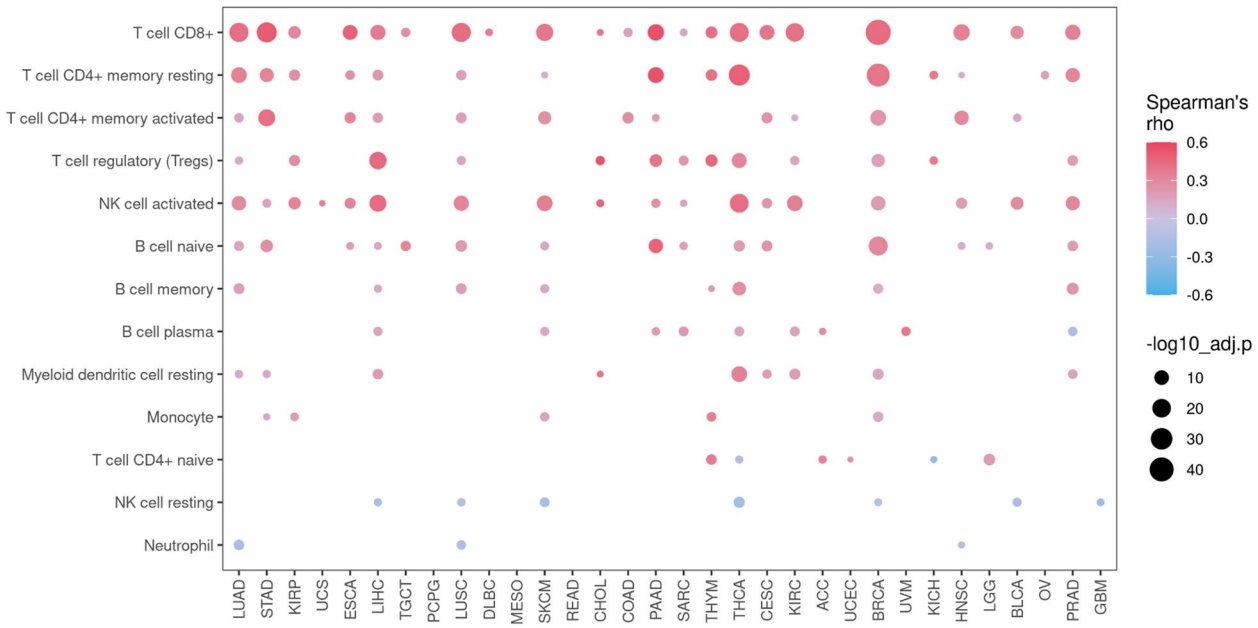

Fig. 4 Relationship between LLT1 expression and immune infiltrates in the TME. Spearman's purity-adjusted correlation coefficient between the infiltration score (estimated by CIBERSORT-ABS from TCGA transcriptomics data) and LLT1 expression is shown in this figure across cancers. The size of the dots represents the adjusted p-values, and the color represents the correlation coefficient

Correlation of LLT1 with tumor genomic features such as TMB, MSI, and MMR

We next examined the relationship between LLT1 expression and tumor genomic markers across cancer types. Tumor mutational burden (TMB) is a measure of the immunogenicity of a tumor. TMB was found to be significantly ($p < 0.05$) and positively correlated with LLT1 expression in KICH, COAD, and UCEC (Fig. 6A, left panel). In TGCT and OV, the TMB score was negatively correlated with LLT1 expression (Fig. 6A, left panel). Microsatellite instability (MSI) occurs as a result of a deficiency in DNA mismatch repair genes (MMR) (EPCAM, MLH1, MSH2, MSH6, PMS2) in cancer. MSI scores in PRAD and COAD were significant ($p < 0.05$)

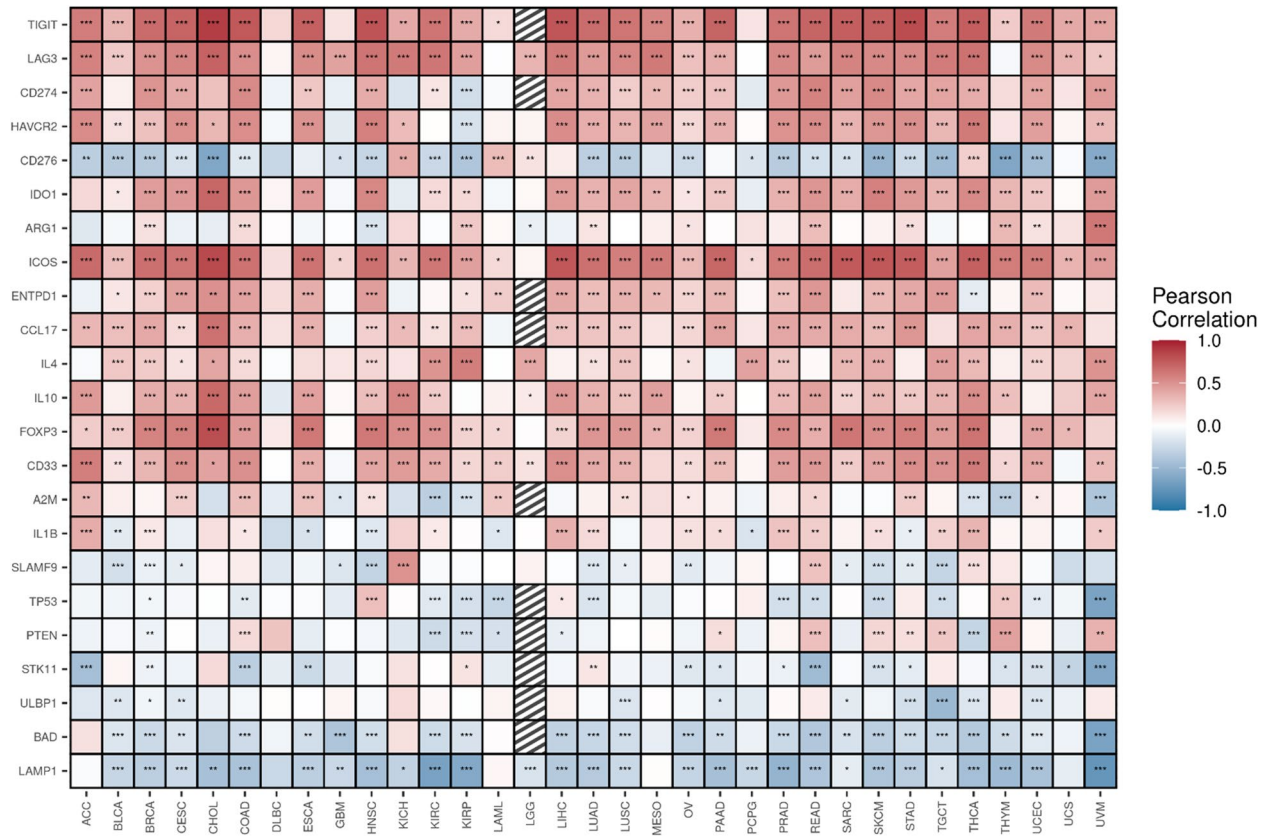

Fig. 5 Correlation of LLT1 expression with expression of immunoregulatory genes. **A** Pearson correlation between relevant immune checkpoint genes and LLT1 expression measured in TPM is shown in this heat map. The thatched tiles represent cases where the correlation coefficient could not be reliably estimated owing to poor data. P-values are coded as follows: * < 0.05, ** < 0.01, *** < 0.001. **B** Individual correlation maps of select immune checkpoint genes are shown. The correlation coefficient (r) values for each gene plot are shown as an inset in each plot. **C** The gene ontology of the positively correlated gene set is shown. The size of the dots represents the level of abundance and the color represents the adjusted p-values

and positively correlated with LLT1 expression, while in TGCT, LAML, BRCA, OV, LUAD, and LUSC, the MSI score was negatively correlated with LLT1 expression (Fig. 6A, right panel). The negative correlations indicate that LLT1 expression is not linked to genomic biomarkers like TMB and MSI in these cancers. An assessment of MMR genes shows a negative association with LLT1 expression in most cancers (Fig. 6B). Interestingly, in COAD and KICH, the deficiency in mismatch repair function in LLT1-high tumors is congruent with the observation of the high MSI and TMB status of these tumors.

LLT1 could be a potential biomarker in patients non-responsive to current ICIs

We have used the CRI iAtlas portal to understand the expression of LLT1 transcripts in patients who did not respond to immune checkpoint therapies across multiple solid cancers. The dataset had information about the clinical outcome of patients in response to different ICI treatments in 5 different cancers, including STAD, BLCA, GBM, KIRC, and SKCM. LT1 We found that a significant proportion of patients among the non-responders in each cancer-treatment group had a high level of LLT1 expression (Fig. 7A). We next examined whether other immune checkpoints and immunoregulatory genes were correlated to LLT1 expression in these groups of non-responding patients. We observed a significant correlation ($p < 0.05$) of LLT1 expression with multiple immune checkpoint genes in certain groups of non-responding patients across cancer indications (Fig. 7B). The SKCM-nivolumab non-responders had the greatest number of genes significantly correlated ($P < 0.01$) with LLT1, including TIGIT, LAG3, CD274 (PD-L1), IDO1, ICOS, ENTPD1, IL10, and FOXP3. This was followed by the KIRC-nivolumab and BLCA-atezolizumab groups, where there were 6 significant correlated genes ($p < 0.05$) from this subset. Interestingly, in GBM, there was a significant correlation ($p < 0.01$) of LLT1 expression with LAG3

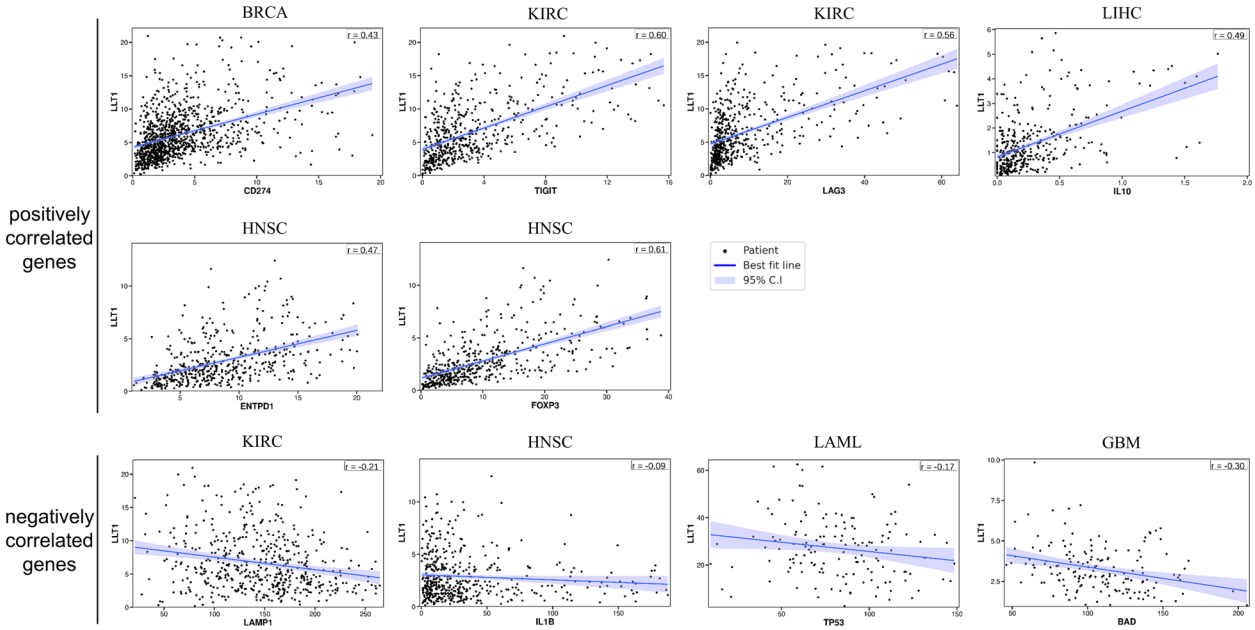

Fig. 5 continued

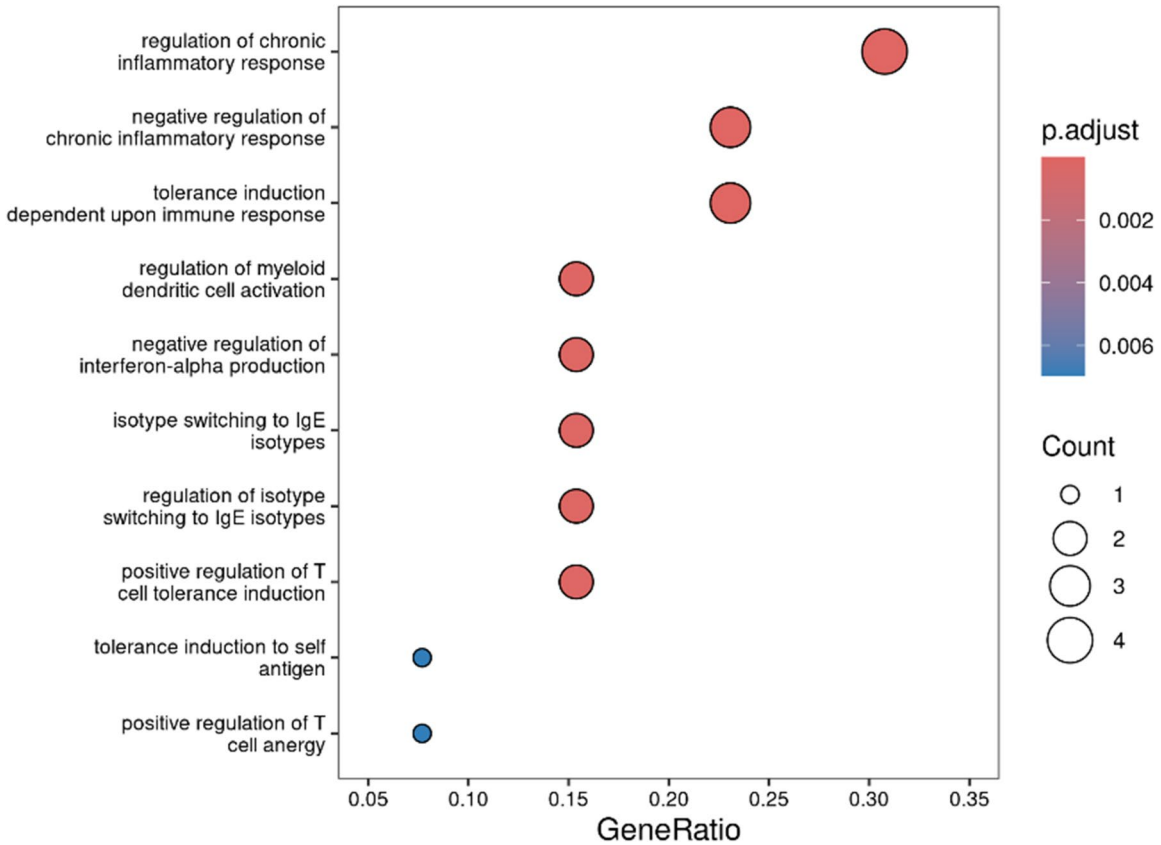

Fig. 5 continued

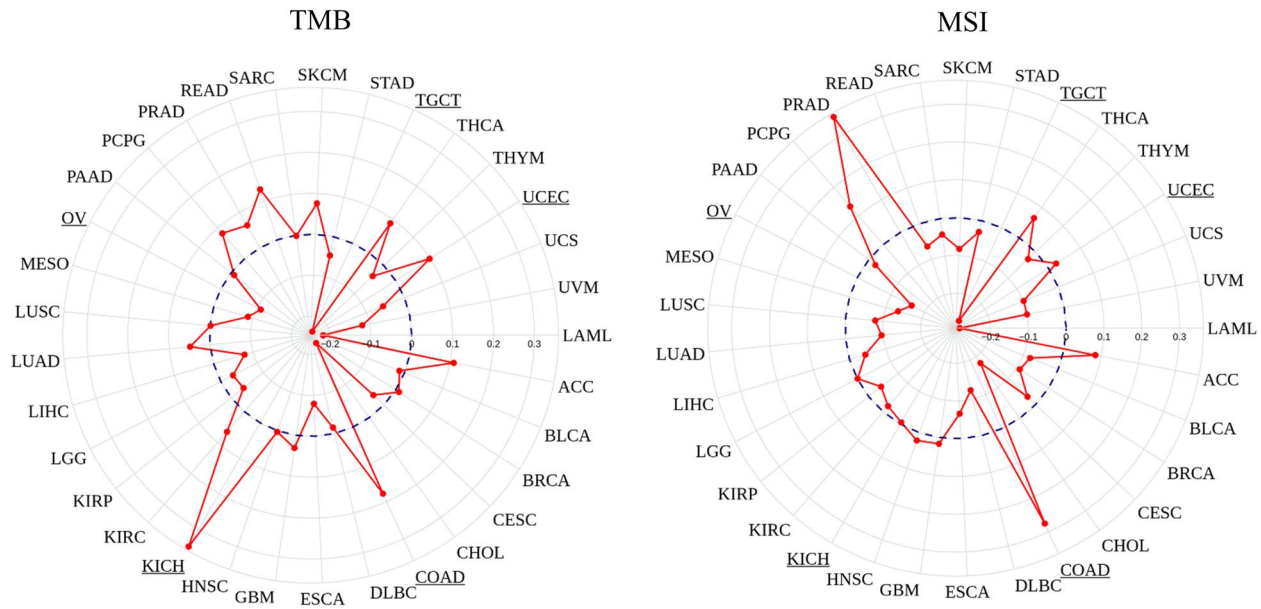

Fig. 6 Correlation between LLT1 expression and tumor genomic markers. **A** Pearson correlation between LLT1 expression in TPM and TMB score is shown in this radar plot. Cancers where the correlation is significant ($p < 0.05$) are *underlined* in the plot (KICH, COAD, OV, TGCT, UCEC). **B** Pearson correlation between LLT1 expression in TPM and MSI score is shown in this radar plot. Cancers where the correlation is significant ($p < 0.05$) are *underlined* in the plot (PRAD, TGCT, LAML, BRCA, COAD, LUAD, LUSC, OV). **C** Pearson correlation between mismatch repair genes and LLT1 expression is shown in this figure. P-values are coded as follows: * < 0.05, ** < 0.01, *** < 0.001

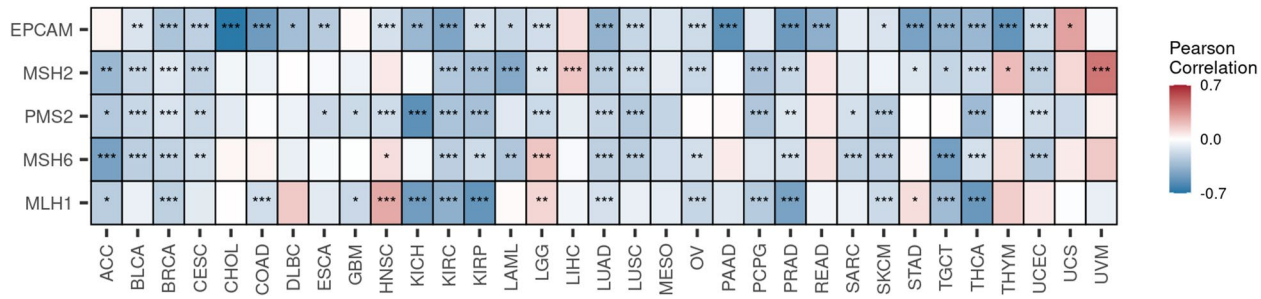

Fig. 6 continued

and CD276 (B7-H3) genes, suggesting potentially new therapeutic options in addition to existing ICIs like pembrolizumab. Taken together, these results suggest that in certain non-responder populations, LLT1 may work in concert with other immune checkpoints and immunoregulatory genes to create an immunosuppressive TME.

Validation of LLT1 expression in certain cancers

We selected specific cancer cell lines to validate our in silico analysis, based on TCGA and clinical datasets. These included immune-resistant prostate cancer cell lines (hormone-refractory PC3, hormone-sensitive DU145, and 22Rv1), glioma cell line (LN229), ovarian cancer cell line (SK-O-V3), and an immune-sensitive liver cancer cell line (Hep G2) [19]. To confirm the specific binding of our anti-LLT1 antibody (4C7), we used CHO-K1 cells transfected with human LLT1 antigen (Fig. 8A; Fig. S4). The results showed cell surface staining indicating LLT1 expression on transfected CHO-K1 cells, while the control (untransfected) CHO-K1 cells showed no staining. In the tumor cell lines, we observed varying levels of LLT1 expression on the cell surface (Fig. 8B; Fig S5). Among the immune-resistant cancers, predominant cell surface expression of LLT1 was observed in prostate cancer cell lines (PC3, DU145, and 22Rv1) and glioma cell lines (LN229) (Fig. 8B, right panel; Fig. S5), validating our findings from the TCGA and clinical datasets.

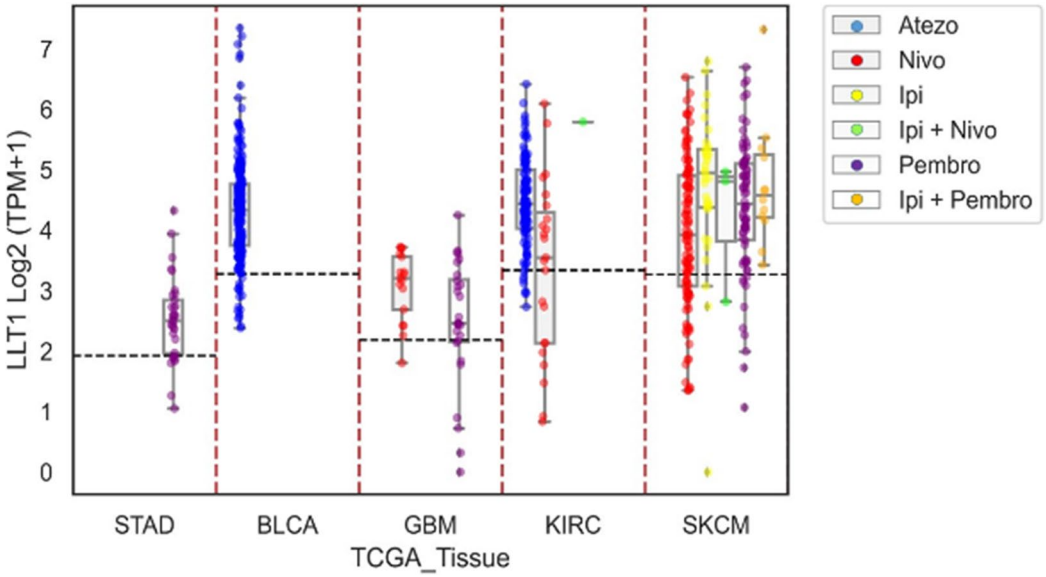

Fig. 7 LLT1 expression and correlation with immune regulation in ICI non-responders. **A** The expression of LLT1 in each non-responsive patient is divided by the drug used to treat the patient and the tissue type. The horizontal dotted lines indicate the median LLT1 value of the pooled dataset as described in the method's section. **B** The topmost axis indicates the cancer under consideration. The second from the top axis indicates the drug to which the patients were unresponsive. The tiles are colored according to the hypergeometric overlap test's p-value. The y-axis indicates the immune genes used in the overlap analysis along with LLT1. P-values are coded as follows: * < 0.05, ** < 0.01, *** < 0.001

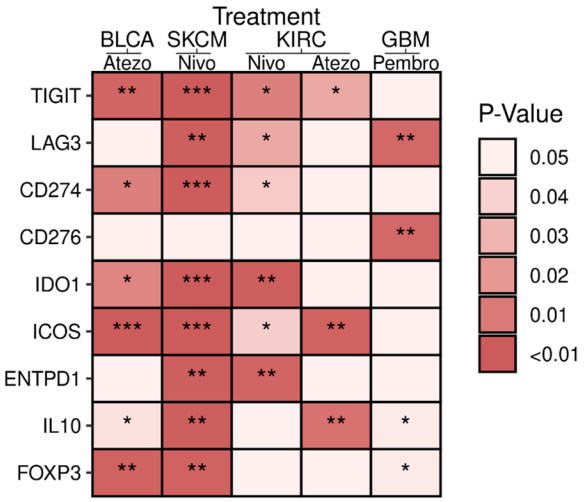

Fig. 7 continued

The immune-sensitive liver cancer cell line (HepG2) also showed robust cell surface LLT1 expression (Fig. 8B, right panel; Fig S5), confirming our TCGA database analysis. However, the immune-resistant ovarian cancer cell line (SK-O-V3) showed low cell surface expression of LLT1 (Fig. 8B, right panel; Fig S5). These results further suggest utilizing LLT1 as a potential therapeutic target in immune-resistant tumors.

Discussion

Biomarker-informed cancer immunotherapy is urgently needed for treating patients with advanced cancer. Currently approved immunotherapies mainly target immune checkpoint pathways like PD-1, PD-L1, and CTLA-4. Recent therapeutic approaches have emerged that target new immune checkpoints such as NKG2A, which is an inhibitory NK cell receptor [20], and other co-inhibitory receptors such as TIGIT, LAG3, and TIM3 [21]. The

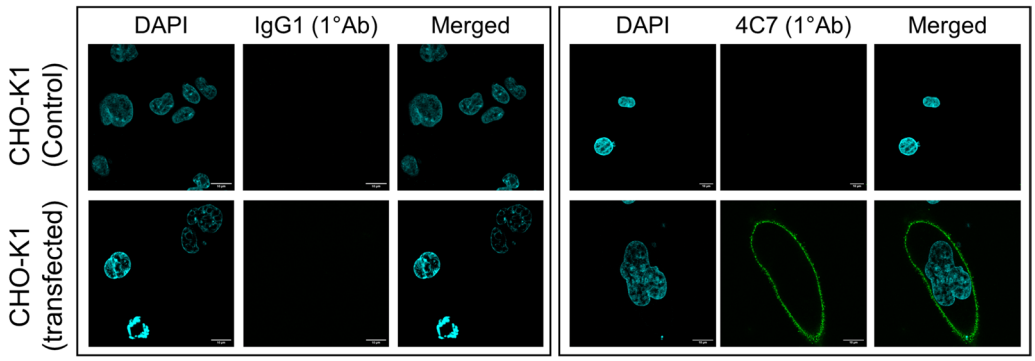

Fig. 8 The expression of LLT1 in different cell lines by confocal microscopy. **A** The surface expression of LLT1 was examined using confocal microscopy. An anti-LLT1 antibody (4C7) was used to probe the cells. DAPI was used for counterstaining the nucleus. The left panel shows cells treated with a secondary antibody attached to a fluorescent probe (Alexa Fluor 488 goat anti-mouse IgG), while the right panel shows cells treated with the anti-LLT1 antibody (4C7) followed by the secondary antibody attached to a fluorescent probe. The green color indicates the binding of the anti-LLT1 antibody to the target antigen on respective cell lines. The binding signal of the anti-LLT1 antibody (green color) was observed only in LLT1 transfected CHO-K1 cells (right panel), while no binding was detected in untransfected CHO-K1 (control) cells (left panel). The scale bar for both panels is 10 µm. **B** The surface expression of LLT1 on different tumor cell lines, including prostate cancer (hormone-refractory PC3, hormone-sensitive DU145, and 22Rv1), liver cancer (Hep G2), glioma (LN229), and ovarian cancer (SK-O-V3), was also investigated. DAPI was used for counterstaining the nucleus, while the same anti-LLT1 antibody (4C7) followed by secondary antibody with the fluorescent probe (Alexa Fluor 488 goat anti-mouse IgG) were used to probe the cells. The green color indicates the binding of the anti-LLT1 antibody to the target antigen on respective tumor cell lines. The scale bar for both panels is 10 µm

identification of NKG2A as a novel immune checkpoint has drawn considerable interest in NK cell targets for cancer immunotherapy. LLT1-CD161 is one such inhibitory NK cell receptor-ligand pair that is known to block NK cell function in various cancers [7]. Existing literature highlights the significance of the CD161-LLT1 interaction in regulating cancers [1, 6], but the precise role of LLT1 is still far from being clearly understood. Here, we conducted a pan-cancer analysis utilizing the TCGA database to understand the role of LLT1 in the tumor microenvironment and how it may facilitate cancer growth and metastasis.

We assessed the differential expression of LLT1 in 33 cancers and found upregulation of expression in 12 cancers, including BRCA, CHOL, ESCA, GBM, HNSC, KIRC, KIRP, LIHC, LUAD, STAD, SARC, and PCPG. Interestingly, in a subset of these cancers, including LIHC, BRCA, HNSC, and LUAD, we observed LLT1 expression to be higher in all pathological stages of the cancer compared to their respective normals. This is consistent with previous studies where high LLT1 expression was observed in these same tissue types [6, 7, 10, 18]. The highest absolute expression of LLT1 was observed in two hematological cancers: DLBC and LAML, suggesting LLT1 to be more prominent in leukemias. In comparison, low levels of LLT1 expression were observed in cancers such as ACC, KICH, and READ.

We found that LLT1 expression levels were related to genetic and epigenetic changes in 33 different types of cancers. Genetic changes such as heterozygous amplification or deletion were the most common type of CNV found in these cancers, and this was linked to LLT1 expression in a significant number of cases. Similarly, epigenetic changes such as methylation levels were found to be linked to LLT1 gene expression, with a large subset of cancers exhibiting low methylation levels and higher LLT1 expression. These findings support previous studies that have suggested a close relationship between abnormal DNA methylation and human cancers [22]. It is noteworthy that LLT1 expression is linked to poorer survival rates in KIRC, KICH, and COAD, where these cancers exhibit lower methylation levels. Low levels of methylation in certain cancers can lead to their progression and severity. Additionally, in meningioma, the subgroup of immunogenic tumors showed increased LLT1 expression. This group is also associated with an influx of immune cells, mainly T cells that are in an exhausted state. Targeting LLT1 with antibodies, as it regulates NK cells, could offer treatment opportunities for remission in this subtype of meningioma patients.

To understand the prognostic significance of elevated LLT1 expression, we performed a univariate Cox proportional regression analysis of LLT1 in pan-cancer. The results indicated that among the cancers that have differential LLT1 expression, LLT1 is a risk factor for survival in patients with COAD, KICH, and KIRC, suggesting LLT1 to be a potential immune checkpoint target in these cancers. On the other hand, LLT1 acts as a protective factor in certain cancers, such as HNSC, LUAD, and BRCA. However, as seen with HNSC, this outcome

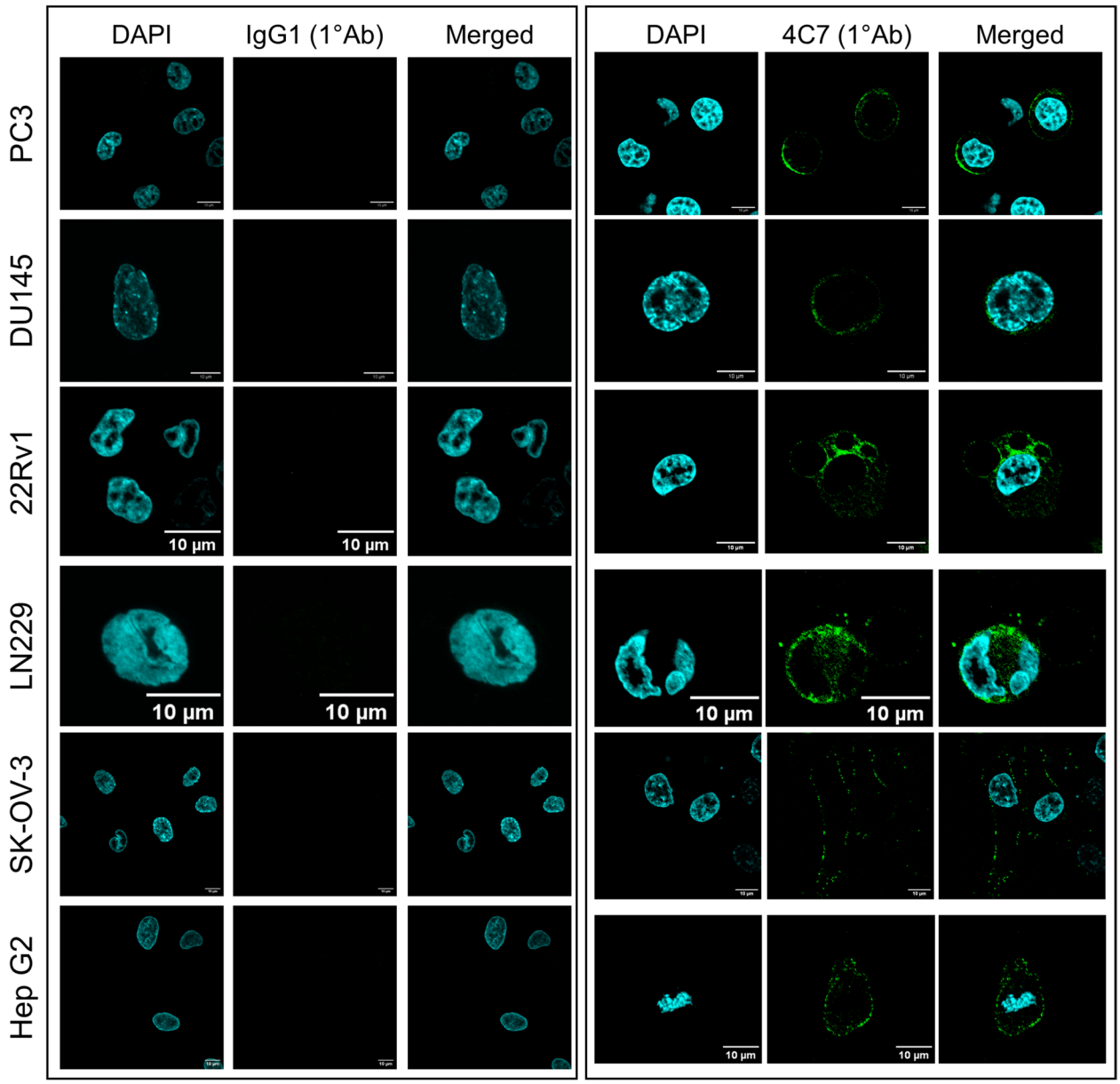

Fig. 8 continued

can vary depending on the histological subtype of the tumor [9, 18]. The observation in LUAD, an NSCLC subtype, is consistent with previous studies where higher LLT1 expression was associated with favorable survival outcomes in this cancer [6]. Notably, in the same study of NSCLC patients, LLT1 expression was limited to the immune cells within the tumor tissue. Therefore, the correlation between LLT1 expression on tumor cells and patient response will require in-depth studies involving single-cell RNA transcriptome analysis of tumor tissue. Thus, it is crucial to perform other analyses that look into the complex interaction of LLT1 within the TME.

Through GSEA of LLT1 using HALLMARK terms, we found that the LLT1 high expression group was linked with pathways related to immune regulatory processes, tumor growth, and metastatic spread of cancer. This further supports previous studies showing LLT1 to be a critical immune regulator and a driver of tumor growth in cancers [23, 24]. Tumors can be categorized as immune-sensitive and immune-resistant, depending on their response to ICIs. An immune-sensitive

tumor is associated with a higher abundance of tumor-infiltrating T lymphocytes (TILs) in the TME, while an immune-resistant tumor is devoid of such TILs [25]. In the context of LLT1's regulatory role in the TME, we investigated how LLT1 expression was associated with immune infiltration. We found effector and cytotoxic immune infiltrates such as CD8+, CD4+T cells, and NK cells to be enriched in certain cancers like BRCA, ESCA, KIRC, KIRP, LIHC, LUAD, and STAD with upregulated LLT1 expression. A strong correlation of these immune infiltrates was also observed in PRAD and SKCM, two cancers without significant upregulation of LLT1 expression. Interestingly, LLT1 expression was positively correlated with infiltration of immunosuppressive Treg cells in LIHC, BRCA, KIRC, and KIRP. This suggests that despite the presence of effector immune cells in these cancers, their activity is countered by cell types driving immune repression.

To further understand the functioning of these immune cells in the TME across cancer types, we looked at the expression levels of various immune checkpoint and oncogenic driver genes and their association with LLT1 expression. We found several immunosuppressive markers like CD274 (PD-L1), TIGIT, LAG3, IDO1, ENTPD1 (CD39), IL10, and FOXP3 to be significantly correlated with high LLT1 expression across almost all 33 cancers. This suggests that despite the presence of TILs, these immune cells are exposed to other mechanisms of inhibition in the TME. This comes in the form of cells being in a state of exhaustion, anergy, or tolerance, also evident from the co-expression of other immunosuppressive cytokines and markers in this milieu. In line with these observations, we also found pro-inflammatory genes or tumor suppressor genes to be downregulated in such cancers. Additionally, the GSEA of LLT1 based on this immune checkpoint gene set indicated an association with immune-related pathways including T cell regulation, myeloid cell activation, and inflammatory signals. These results together hint towards LLT1 playing a role in promoting an immune-resistant TME, often associated with 'cold' tumors. Notably, in cancers like GBM, PAAD, and PRAD, which are often referred to as immune-resistant 'cold' tumors [26–30], targeting LLT1 could be a potential strategy to relieve immune suppression.

Examination of the association of genomic features showed a significant positive correlation of LLT1 expression with TMB in COAD, KICH, and UCEC and a positive correlation with MSI in COAD and PRAD. Also, LLT1 expression was associated with MMR-deficient (MMRd) status in almost all cancers, specifically colon (COAD) and kidney (KICH) tumors. This relationship between LLT1 and genomic biomarkers suggests an approach where these biomarkers can be combined with anti-LLT1 antibodies in clinical trials to further improve response rates in tumors.

We wanted to investigate gene correlations between LLT1 and response to current ICI treatments. We observed that across all cancer-treatment groups, a significant proportion of non-responding patients had LLT1 expression that was above the expression median of that respective group. The proportions of non-responders with above median LLT1 expression levels were high in GBM (40%) and KIRC (~90%), indicating that high LLT1 expression could potentially be a mechanism of resistance in these non-responders. With this observation, we next determined whether other established immune checkpoints were upregulated in the same non-responding patient populations. Among the cancer-treatment groups with high LLT1 expression, there was a subset where multiple immune checkpoint genes correlated with LLT1 expression. The SKCM-nivolumab group had the highest number of correlated immune checkpoints, followed by the KIRC-nivolumab and BLCA-atezolizumab groups. Interestingly, in the GBM-pembrolizumab group, immune checkpoints such as LAG3 and CD276 (B7-H3) were correlated with LLT1 expression. As alluded to earlier, GBM is an immune-resistant 'cold' tumor where current immunotherapies offer minimal benefit to the larger patient population. Existing immune checkpoints that are being targeted in GBM include CD274 (PD-L1), LAG3, and CD276 (B7-H3) [31, 32]. Therefore, antibodies targeting LLT1 could be a potential therapeutic option in GBM patients non-responsive to existing ICIs. Alternatively, anti-LLT1 antibodies may be combined with one or more immune checkpoint targets shown to be strongly associated with LLT1 in terms of gene expression. This strategy can potentially boost patient responses in indications like SKCM, KIRC, BLCA, and GBM, providing additional therapeutic options to a cohort of non-responder patients.

Finally, we analyzed specific cancer cell lines to experimentally validate our findings from the publicly available genomic and clinical databases. LLT1 was expressed in immune-resistant tumor cell lines, predominantly in prostate cancer and glioma, and although low, was clearly detected in ovarian cancer, indicating a trend of upregulated LLT1 expression in immunologically "cold" tumors. These findings are consistent with previous studies in the literature [7, 8, 33] and suggest that LLT1 could be a potential therapeutic target in immune-resistant tumors.

There has been significant progress made in developing predictive biomarkers for ICIs, leading to better patient screening and improvements in treatment efficacies. The predictive biomarkers approved in the clinic include PD-L1 expression determination, MSI/ MMRd testing, and TMB measurement [34]. PD-L1 expression

levels have been used to assess responses to anti-PD1-1 and anti-PD-L1 therapies in NSCLC, HNSCC, ESCA, cervical, and bladder cancers [35]. MSI/ MMRd testing has been shown to predict responses to anti-PD-1 and anti-CTLA-4 combination therapies in patients with metastatic colorectal cancer [36]. High TMB scores were shown to favorably affect responses to anti-PD-1 and anti-CTLA-4 combination therapies in NSCLC, melanoma, and bladder cancers [37]. In addition, new prediction metrics like tumor-infiltrating lymphocytes (TILs) and gene expression profiles (GEPs) are being developed to evaluate tumoral responses to ICIs. Infiltration of TILs such as CD8+and CD4+T cells in the TME is associated with improved responses to ICIs in various cancer types [38]. In the POPLAR trial, GEPs including a 10 gene 'IFN-γ signature' pattern were analyzed in progressive NSCLC patients receiving atezolizumab. It was observed that a high level of this 'IFN-γ signature' pattern was correlated with improved overall survival (OS) in these patients [39]. Such biomarkers play a key role in determining patient response to ICI therapies in different malignancies. Therefore, basic research can identify new biomarkers for clinical translation. In this study, we have shown that LLT1 is co-expressed with various immune checkpoint genes and genomic features to drive an immunosuppressive TME. Also, LLT1 expression shows favorable association with patient prognosis in various cancer types. Based on these observations, LLT1 holds promise to be a potential predictive biomarker in different cancer types.

This study represents one of the initial analyses where LLT1 was examined in silico across all types of cancers. It is important to acknowledge certain limitations. The pan-cancer expression analysis used tumor samples mainly from the TCGA database, which includes both primary and metastatic tumors. It is essential to consider that primary and secondary tumors have different biological characteristics, potentially impacting the results of the analysis if they had been examined separately. Having access to public databases containing complete staging information for all cancers in the future would allow us to address this issue.

Although we established a relationship between LLT1 expression and immune infiltration in multiple tumors, it should be noted that this was achieved using the computational algorithm CIBERSORT, which has its own limitations. These limitations include: (i) using predefined gene expression signatures that, if incomplete or inaccurate, could bias the deconvolution results, (ii) the inability to detect rare cell types due to their low abundance in tumor samples, (iii) potential batch effects and technical biases in the gene expression data that could confound the deconvolution results, and (iv) the inability to capture the functional states of immune cells, instead providing estimates of immune cell populations.

In the future, it will be necessary to employ additional scientific techniques to experimentally validate these findings. This could involve using single-cell RNA sequencing (scRNA) of tumor biopsies to gain further insight into the role of LLT1 in both immune and tumor compartments. It could also involve the use of multiplex immunohistochemistry (mIHC) to enable simultaneous detection and quantification of LLT1 and other related biomarkers in the tumor microenvironment (TME). Additionally, liquid biopsies from patients could prove useful in determining the effect of LLT1 on peripheral blood markers.

Furthermore, we demonstrated the correlation between LLT1 gene expression and survival, as well as its association with several immune gene signals. However, the prognostic value of LLT1 in immune evasion requires further exploration. Subsequent analyses in independent clinical datasets could verify these findings. Finally, comprehensive and individualized adaptive clinical trials would be necessary to guide the selection and validation of such novel biomarkers.

The overall findings of this study suggest that gene signatures exhibiting immune-resistant TME are associated with upregulated LLT1, as seen from both TCGA analysis and a subset of ICI-resistant tumors (Fig. 9, upper panel). This data provides a better understanding of the TME in patient tumors and could lead to new therapeutic options for cancer patients. It is hypothesized that a significant fraction of non-responsive patients would benefit from targeted therapies such as an anti-LLT1 monoclonal antibody that can disrupt the LLT1-CD161 interaction. Previous studies have shown the effectiveness of such strategies of LLT1 blockade in selective 'cold' tumors. LLT1 blockade, through the use of an anti-LLT1 antibody, has been shown to restore NK cell-mediated cytotoxicity in prostate cancer cells [7]. On the other hand, small interfering RNA (siRNA)-mediated downregulation of LLT1 led to increased NK cell-mediated lysis of glioma cells [8]. A new weapon in the arsenal could be our lab's newly developed anti-LLT1 monoclonal antibody ZM008, which has been recently approved for a first-in-human phase I study and is scheduled to go into clinical trials soon [40–42] (Fig. 9, boxed panel). Altogether, this study will help clinicians (a) identify potential patients for the upcoming first-in-human clinical trials with ZM008 and (b) develop a predictive scoring system for patient prognosis. We believe that new immunotherapy approaches using LLT1 blockade or a combination of LLT1 blockade and other existing ICIs could be highly effective against immune-resistant 'cold' tumors.

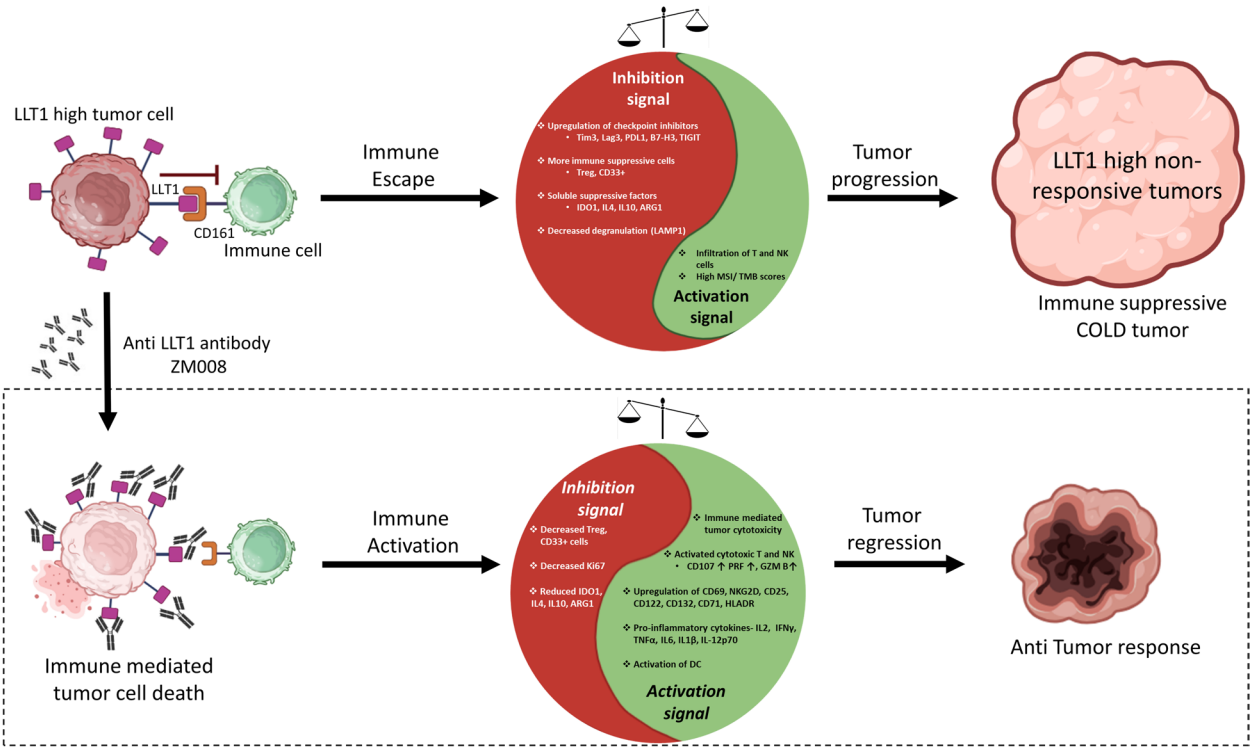

Fig. 9 Summary of LLT1's role in TME of cancers and possible implications for therapy. Interaction of LLT1 with CD161 on immune cells like T cells and NK cells impairs their anti-tumor activity, leading to immune escape and tumor progression. As our study suggests, high LLT1 expression is associated with various inhibitory signals in the TME, as shown in the yin-yang-like representation in the top panel. These inhibitory signals induce immune dysfunction, thereby creating a TME conducive to immune-resistant "COLD" tumors. Blocking the inhibitory LLT1-CD161 axis could shift the balance towards immune activation, mediating immune cell-mediated killing of tumors and prompting tumor regression. Anti-LLT1 antibody ZM008 could provide a potential treatment option for these immune-resistant tumors. This antibody drug could potentially transform the TME into an immune-responsive "HOT" tumor. The boxed panel in the figure indicates the proposed hypothesis of this prospective anti-LLT1 antibody-based immunotherapy approach

Conclusions

Our study suggests that LLT1 expression is upregulated in several human cancers and is associated with different patient survival outcomes. Our findings also demonstrate an association between LLT1 expression and numerous immunosuppressive markers in the tumor microenvironment (TME) of multiple cancers. Taken together, these results offer further insights into the potential role of LLT1 in cancer development and progression, especially in immune-resistant tumors. LLT1 may be a promising therapeutic target in such cancers and could provide additional benefits to patients beyond the current ICI treatment options.

Methods

Pan-cancer LLT1 expression

Datasets were downloaded from the UCSC Xena project [43]. 33 TCGA cohorts in the GDC Hub category were used (https://xenabrowser.net/datapages/). From each cohort, the "HTSeq – FPKM" data file was downloaded from each of the TCGA cohorts. The expression value for each gene in a given patient was converted from $\log_2$ (FPKM + 1) (Fragments Per Kilobase Million) to $\log_2$ (TPM + 1) (Transcripts Per Million) using the following formula:

$$TPM_i = \frac{FPKM_i}{\sum_j FPKM_j} \times 10^6$$

Where the index j indicates a summation of all the genes measured for a given tumor sample in a single experiment, the distribution of the logarithms of the TPM + 1 values of LLT1 for each of the 33 cancer types was visualized using box plots. The Mann-Whitney test (two-sided) was used to compare the logarithm of the expression value (TPM + 1) between the tumor and adjacent normal in cancers where both of these data were available. This was done using *ggplot2* [44] and *ggstats* [45] in *R* software v4.2.3 [46]. For validation, data were downloaded and analyzed for each tumor cell line from the CCLE database (https://sites.broadinstitute.org/ccle/).

Stage-wise LLT1 expression in certain cancers

The distribution of the logarithms of the *(TPM + 1)* values of LLT1 for each stage (AJCC Pathologic Stage) was visualized using box plots. The staging information was obtained from clinical files from the TCGA GDC portal for each cancer project specifically: https://portal.gdc.cancer.gov/. The Mann-Whitney test (two-sided) was used to compare the logarithm of the expression value plus one between the tumor and adjacent normal. GraphPad Prism 7.01 was used for data analysis.

Survival regression

Univariate Cox-Proportional Hazards regression was performed for overall survival using LLT1 expression (TPM) as the independent regression variable. The survival data was obtained from the UCSC Xena project, and the analysis was performed using the Lifelines package in Python 3.8 [47]. Hazard ratios and their 95% confidence intervals were computed and visualized as interval plots. *Kaplan Meier Curves*: The 50 percentile value of the LLT1 expression was taken as the cut-off to divide patients into LLT1 high expression and LLT1 low expression groups. Kaplan Meier curves were plotted, and the log-rank test was performed to test the hypothesis that they are distinguishable and separable. This analysis was performed using the *survival* package in *R 4.2.3* [48, 49]. For validation, datasets were downloaded and analyzed from the PRECOG database (https://precog.stanford.edu/).

GSEA of KEGG Hallmark of Cancer pathways with LLT1

The "Hallmarks of Cancer" gene sets represent a collection of biological processes and characteristics that are commonly observed in cancer cells [50]. The data from each cancer from the TCGA database was filtered, and only tumor data was carried forward for further analysis. Following this, the patient records were rank-ordered based on the level of expression of LLT1. The top 30% and bottom 30% of the data were separated as two groups, and differential expression analysis was carried out using the *PyDeSeq2* python package [51, 52]. 50 gene sets collectively termed as the "Hallmark Gene sets" were acquired from the *MSigDB* site (https://www.gsea-msigdb.org/gsea/msigdb). The *GSEApy* package was used to carry out gene set enrichment analysis for the different hallmark gene sets using the differentially expressed genes between the two groups [53].

Correlation of Immune Infiltration measures with LLT1

CIBERSORT is a computational algorithm that enables quantifying the proportions of different immune cell types within a complex mixture of cells, such as a tumor biopsy sample, based on gene expression data [54]. Using the *TIMER2* web server (http://timer.cistrome.org/) hosted immune infiltration analysis tool, the purity-adjusted Spearman's correlation of immune cell infiltration score (as estimated by *CIBERSORT-ABS*) was computed, and its correlation with LLT1 expression in 33 cancers from the TCGA database was evaluated [55]. The resulting bubble plot was bi-clustered according to the correlation values using the spectral co-clustering algorithm from *scikit-learn 0.16.1*, with the *'n_clusters'* parameter chosen heuristically to be 3 [56].

Correlation of Immune-related genes with LLT1

The Gene Ontology Resource (Gene Ontology Resource) was used for obtaining the gene list for specific pathways [57]. The ontology section of the database states the GO term of interest, including 'T cell activation', 'cytokine involved in immune response', or 'NK cell activation'. The 'Biological Process' of the database was used in shortlisting candidates from a long gene list using the ontology search of the selected GO terms deemed relevant to predict the immunotherapy response. From these shortlisted gene candidates, we further pruned the dataset to include a subset of genes that have been extensively studied and have an established role in anti-tumor immunity.

The gene correlations for LLT1 and this set of selected genes from the TCGA-GDC datasets across cancers were calculated using the Pearson correlation function. The significance level associated with the estimate of the correlation coefficients is indicated by the star marks on the tile of the heat map. The resulting correlation matrix was then bi-clustered using the spectral co-clustering method as implemented in the *scikit-learn 0.16.1* package with hyperparameter '*n_cluster*' set to value 5 heuristically. The genes that are significantly ($p < 0.05$) correlated to LLT1 across all cancers consistently can be identified by visual inspection of the heat maps. Gene ontology analysis was run on these selected sets of genes to identify their role with greater specificity using the *enrichGO* function in the *ClusterProfiler* package in *R v4.2.3* [58, 59].

Genomic marker correlation with LLT1

Tumor Mutational Burden (TMB) is computed as the number of non-synonymous mutations per megabase (Mb) of the genome sequenced. *MAF* files for each of the 33 cancers from the TCGA database were queried using the *TCGAbiolinks* package in *R* version 4.2.3 [60–62]. Tumor mutational burden was computed for each patient using the *tmb* function in the *maftools* package in R [63]. The Pearson correlation coefficients of these TMB scores with LLT1 expression was computed for all cancers. Precomputed MSI scores of TCGA patient samples were obtained from the *MSIsensor.10k* data frame using the

BiocOncoTK package in R version 4.2.3 [64]. The Pearson correlation coefficient of these MSI scores and LLT1 expression was computed. Both these pan-cancer correlation data were visualized in a radar chart format using Python 3.8. Additionally, Pearson correlation between LLT1 expression and DNA mismatch repair (MMR) genes, *EPCAM*, *MLH1*, *MSH2*, *MSH6*, and *PSM2*, was computed across all cancers.

Cell culture

The control cell line, CHO-K1, was cultured in DMEM/F12 media, 15 mM HEPES with 10% Fetal Bovine Serum (FBS), and 1% Penicillin-Streptomycin. The tumor cell line, PC3, was cultured in DMEM/F12 media with 20% FBS, 1mM Sodium Pyruvate, and 1% Penicillin-Streptomycin. Tumor cell lines, 22RV 1, DU145, and SK-OV-3 were cultured in RPMI 1640 media with 10% FBS, 1X Sodium Pyruvate, and 1% Penicillin-Streptomycin. Other tumor cell lines, Hep G2, and LN229 cell lines, were cultured in DMEM/F12 media with 10% FBS, 1mM Sodium Pyruvate and 1% Penicillin-Streptomycin. All the cell lines were maintained in a 37 °C incubator with 5% CO_2.

Immunofluorescence staining to detect LLT1 expression

Control (CHO-K1) and respective tumor cells were grown on glass cover slips in their respective cell culture medium. Cells were washed with 1X PBS buffer, then fixed in 2% formaldehyde in PBS for 30 s at room temperature (RT). Cells were then rinsed twice with 1X PBS, followed by blocking with 5% BSA for 1 h at RT. Following this, incubation with 2 µg anti-LLT1 antibody (4C7) was carried out for 1 h at RT, and then cells were washed three times in 1X PBS buffer. Cells were then incubated with 2 µg Alexa Fluor 488 goat anti – mouse IgG1 for 1 h at RT followed by three times washing in 1X PBS buffer. Cell nuclei were stained using DAPI (1:1000 for 5 min at RT). Cells were then rinsed thrice in 1X PBS buffer and left in 1X PBS buffer until imaging. Immunofluorescence microscopy was performed on the Olympus FV3000- 4 laser scanning confocal microscope with a 60X magnification, 1.35-NA objective. Cells were observed and imaged by using appropriate wavelengths (for DAPI, λex: 405 nm and λem: 430–470 nm; for Alexa 488, λex: 488 nm and λem: 510–530 nm). Images were finally analyzed with the Fiji/ ImageJ software.

Overlap analysis of upregulated LLT1 non-responder population with select upregulated immune checkpoint gene non-responder population

Transcriptomics data, paired with patient-wise information on immunotherapy response and name of drug used, was downloaded from the CRI iAtlas portal's associated file repository on https://www.synapse.org/ (SYN-ID: "syn24200710") [65]. This dataset contained transcriptomics data in TPM for GBM, STAD, KIRC, BLCA, and SKCM. For each cancer indication, a tissue type-wise median LLT1 expression was computed by combining the TCGA data and this iAtlas data.

Using this median from the pooled data, the patients who were classified as non-responders to immunotherapy in the "Non-responder" column of the clinical dataset from iAtlas were classified into three following sets:

a. All non-responders who have LLT1 expression above the median of LLT1 expression in the tissue-specific pooled dataset as mentioned earlier.
b. All non-responders who have a given gene *i* above the median of the gene *i* in the tissue-specific pooled dataset as mentioned earlier.
c. All non-responders who have LLT1 expression above the median of LLT1 expression and all non-responders who simultaneously have a given gene *i* above the median of the gene *i* in the tissue-specific pooled dataset as mentioned earlier.

The number of patients in the three sets was noted, and the tissue-wise set of all non-responders was taken as the superset of these three. Set C is the intersection of sets A and B. The gene *i* is a member of the set of all genes used in the correlation analysis of LLT1 previously. A hypergeometric overlap test was done to see if this overlap was by pure chance or not. This was done to show that there exists a sub-population of ICI non-responders whose patients are simultaneously high in LLT1 and another immune checkpoint gene, which could indicate that they might be potential candidates for LLT1 blockade therapy alone or in combination with immune checkpoint blockade (ICB).

Supplementary Information

The online version contains supplementary material available at https://doi.org/10.1186/s12885-024-13074-z.

Additional file 1. Table S1. Mapping respective cancers from CCLE to TCGA.

Additional file 2. Fig. S1. LLT1 expression profiles across different tumors in the TCGA and CCLE databases. Comparative expression of LLT1 in 24 cancer types from TCGA and CCLE through the Wilcoxon rank sum test.

Additional file 3. Fig. S2.LLT1 expression patterns in different tumor subtypes of meningioma. The expression levels of LLT1 transcripts in different tumor subtypes analyzed through the Mann-Whitney Test. *$P < 0.05$, ** $P < 0.01$, *** $P < 0.001$.

Additional file 4. Fig. S3. Correlation of LLT1 expression with overall survival (OS) in cancers from the PRECOG database. Selected Kaplan-Meier curves of OS in patients with high and low LLT1 expression in two cancers, COAD and KICH, from the PRECOG database.

Additional file 5. Fig. S4. LLT1 expression in CHO-K1 cell lines, represented by larger sized image panels. Select image panels from Fig. 8A are shown again for a clearer fluorescence visualization.

Additional file 6. Fig. S5. LLT1 expression in different tumor cell lines, represented by larger sized image panels. Select image panels from Fig. 8B are shown again for a clearer fluorescence visualization.

Additional file 7. Supplementary Methods.

Acknowledgements
We sincerely thank Dr. Narendra Chirmule, Dr. Ana Anderson, Dr. Karthik Viswanathan, Dr. Andy Rakestraw, Dr. Pradip Majumdar, and Dr. Debasish Roychowdhury for critical reading of the manuscript.

Authors' contributions
TM, SG, and GR contributed equally to this paper.TM, SG, SK, and GR designed research. TM, SG, SK, and GR performed research and analyzed data. AT, AD, SB, YM, and SK performed reviews. TM, SG, GR, MSM, and MG wrote the paper. MSM and MG developed the concept.

Funding
This declaration is "not applicable".

Data availability
The datasets used in this study can be found in the TCGA Research Network (https://portal.gdc.cancer.gov/), CCLE database (https://sites.broadinstitute.org/ccle/), cBioPortal database (https://www.cbioportal.org/), PRECOG (https://precog.stanford.edu/), and iAtlas Explorer (https://www.synapse.org/#!Synapse: syn24200710).

Declarations

Ethics approval and consent to participate
The declaration is not applicable.

Competing interests
TM, SK, AT, AD, SB, YM, and SK are employees of Zumutor Biologics. SG is a former employee of Zumutor Biologics. MG, AT, AD, SB, and YM have stock options in Zumutor Biologics, the company that owns the anti-LLT1 antibody, ZM008. MSM and GR declared no competing interests.

Author details
[1]Zumutor Biologics, Bangalore, Karnataka, India. [2]Indian Institute of Science Education and Research (IISER), Pune, India.

Received: 14 May 2024 Accepted: 17 October 2024
Published online: 07 November 2024

References

1. Braud VM, Meghraoui-Kheddar A, Elaldi R, Petti L, Germain C, Anjuere F. LLT1-CD161 interaction in cancer: promises and challenges. Front Immunol. 2022;13: 847576.
2. Germain C, Bihl F, Zahn S, Poupon G, Dumaurier MJ, Rampanarivo HH, et al. Characterization of alternatively spliced transcript variants of CLEC2D gene. J Biol Chem. 2010;285(46):36207–15.
3. Boles KS, Barten R, Kumaresan PR, Trowsdale J, Mathew PA. Cloning of a new lectin-like receptor expressed on human NK cells. Immunogenetics. 1999;50(1–2):1–7.
4. Skalova T, Blaha J, Harlos K, Duskova J, Koval T, Stransky J, et al. Four crystal structures of human LLT1, a ligand of human NKR-P1, in varied glycosylation and oligomerization states. Acta Crystallogr D Biol Crystallogr. 2015;71(Pt 3):578–91.
5. Germain C, Meier A, Jensen T, Knapnougel P, Poupon G, Lazzari A, et al. Induction of lectin-like transcript 1 (LLT1) protein cell surface expression by pathogens and interferon-gamma contributes to modulate immune responses. J Biol Chem. 2011;286(44):37964–75.
6. Braud VM, Biton J, Becht E, Knockaert S, Mansuet-Lupo A, Cosson E, et al. Expression of LLT1 and its receptor CD161 in lung cancer is associated with better clinical outcome. Oncoimmunology. 2018;7(5): e1423184.
7. Mathew SO, Chaudhary P, Powers SB, Vishwanatha JK, Mathew PA. Overexpression of LLT1 (OCIL, CLEC2D) on prostate cancer cells inhibits NK cell-mediated killing through LLT1-NKRP1A (CD161) interaction. Oncotarget. 2016;7(42):68650–61.
8. Roth P, Mittelbronn M, Wick W, Meyermann R, Tatagiba M, Weller M. Malignant glioma cells counteract antitumor immune responses through expression of lectin-like transcript-1. Cancer Res. 2007;67(8):3540–4.
9. Santos-Juanes J, Fernandez-Vega I, Lorenzo-Herrero S, Sordo-Bahamonde C, Martinez-Camblor P, Garcia-Pedrero JM, et al. Lectin-like transcript 1 (LLT1) expression is associated with nodal metastasis in patients with head and neck cutaneous squamous cell carcinoma. Arch Dermatol Res. 2019;311(5):369–76.
10. Marrufo AM, Mathew SO, Chaudhary P, Malaer JD, Vishwanatha JK, Mathew PA. Blocking LLT1 (CLEC2D, OCIL)-NKRP1A (CD161) interaction enhances natural killer cell-mediated lysis of triple-negative breast cancer cells. Am J Cancer Res. 2018;8(6):1050–63.
11. Germain C, Guillaudeux T, Galsgaard ED, Hervouet C, Tekaya N, Gallouet AS, et al. Lectin-like transcript 1 is a marker of germinal center-derived B-cell non-hodgkin's lymphomas dampening natural killer cell functions. Oncoimmunology. 2015;4(8):e1026503.
12. Schmidt A, Oberle N, Krammer PH. Molecular mechanisms of treg-mediated T cell suppression. Front Immunol. 2012;3:51.
13. Veglia F, Sanseviero E, Gabrilovich DI. Myeloid-derived suppressor cells in the era of increasing myeloid cell diversity. Nat Rev Immunol. 2021;21(8):485–98.
14. Haslam A, Prasad V. Estimation of the percentage of US patients with Cancer who are eligible for and respond to checkpoint inhibitor immunotherapy drugs. JAMA Netw Open. 2019;2(5):e192535.
15. Barretina J, Caponigro G, Stransky N, Venkatesan K, Margolin AA, Kim S, et al. The Cancer Cell Line Encyclopedia enables predictive modelling of anticancer drug sensitivity. Nature. 2012;483(7391):603–7.
16. Nassiri F, Liu J, Patil V, Mamatjan Y, Wang JZ, Hugh-White R, et al. A clinically applicable integrative molecular classification of meningiomas. Nature. 2021;597(7874):119–25.
17. Vasselli JR, Shih JH, Iyengar SR, Maranchie J, Riss J, Worrell R, et al. Predicting survival in patients with metastatic kidney cancer by gene-expression profiling in the primary tumor. Proc Natl Acad Sci U S A. 2003;100(12):6958–63.
18. Sanchez-Canteli M, Hermida-Prado F, Sordo-Bahamonde C, Montoro-Jimenez I, Pozo-Agundo E, Allonca E, et al. Lectin-like transcript 1 (LLT1) checkpoint: a novel independent prognostic factor in HPV-negative oropharyngeal squamous cell carcinoma. Biomedicines. 2020;8(12):535.
19. Wang L, Geng H, Liu Y, Liu L, Chen Y, Wu F, et al. Hot and cold tumors: Immunological features and the therapeutic strategies. MedComm (2020). 2023;4(5):e343.
20. Andre P, Denis C, Soulas C, Bourbon-Caillet C, Lopez J, Arnoux T, et al. Anti-NKG2A mAb is a checkpoint inhibitor that promotes anti-tumor immunity by unleashing both T and NK Cells. Cell. 2018;175(7):1731–43 e13.
21. Anderson AC, Joller N, Kuchroo VK. Lag-3, Tim-3, and TIGIT: co-inhibitory receptors with Specialized functions in Immune Regulation. Immunity. 2016;44(5):989–1004.
22. Saghafinia S, Mina M, Riggi N, Hanahan D, Ciriello G. Pan-cancer Landscape of aberrant DNA methylation across human tumors. Cell Rep. 2018;25(4):1066–80.
23. Sun Y, Malaer JD, Mathew PA. Lectin-like transcript 1 as a natural killer cell-mediated immunotherapeutic target for triple negative breast cancer and prostate cancer. J Cancer Metastasis Treat. 2019;2019:5.
24. Malaer JD, Mathew PA. Role of LLT1 and PCNA as natural killer cell Immune Evasion Strategies of HCT 116 cells. Anticancer Res. 2020;40(12):6613–21.
25. Zemek RM, Chin WL, Nowak AK, Millward MJ, Lake RA, Lesterhuis WJ. Sensitizing the Tumor Microenvironment to Immune Checkpoint Therapy. Front Immunol. 2020;11: 223.
26. Liu Z, Meng Q, Bartek J Jr, Poiret T, Persson O, Rane L, et al. Tumor-infiltrating lymphocytes (TILs) from patients with glioma. Oncoimmunology. 2017;6(2): e1252894.

27. Woroniecka KI, Rhodin KE, Chongsathidkiet P, Keith KA, Fecci PE. T-cell dysfunction in Glioblastoma: applying a New Framework. Clin Cancer Res. 2018;24(16):3792–802.
28. Binnewies M, Roberts EW, Kersten K, Chan V, Fearon DF, Merad M, et al. Understanding the tumor immune microenvironment (TIME) for effective therapy. Nat Med. 2018;24(5):541–50.
29. Bear AS, Vonderheide RH, O'Hara MH. Challenges and opportunities for pancreatic cancer immunotherapy. Cancer Cell. 2020;38(6):788–802.
30. Bilusic M, Madan RA, Gulley JL. Immunotherapy of prostate cancer: facts and hopes. Clin Cancer Res. 2017;23(22):6764–70.
31. Harris-Bookman S, Mathios D, Martin AM, Xia Y, Kim E, Xu H, et al. Expression of LAG-3 and efficacy of combination treatment with anti-LAG-3 and anti-PD-1 monoclonal antibodies in glioblastoma. Int J Cancer. 2018;143(12):3201–8.
32. Tang X, Wang Y, Huang J, Zhang Z, Liu F, Xu J, et al. Administration of B7-H3 targeted chimeric antigen receptor-T cells induce regression of glioblastoma. Signal Transduct Target Ther. 2021;6(1):125.
33. Klijn C, Durinck S, Stawiski EW, Haverty PM, Jiang Z, Liu H, et al. A comprehensive transcriptional portrait of human cancer cell lines. Nat Biotechnol. 2015;33(3):306–12.
34. Duffy MJ, Crown J. Biomarkers for predicting response to immunotherapy with immune checkpoint inhibitors in cancer patients. Clin Chem. 2019;65(10):1228–38.
35. McKean WB, Moser JC, Rimm D, Hu-Lieskovan S. Biomarkers in precision cancer immunotherapy: promise and challenges. Am Soc Clin Oncol Educ Book. 2020;40:e275–291.
36. Overman MJ, Lonardi S, Wong KYM, Lenz HJ, Gelsomino F, Aglietta M, et al. Durable clinical benefit with Nivolumab Plus Ipilimumab in DNA mismatch Repair-Deficient/Microsatellite instability-high metastatic colorectal Cancer. J Clin Oncol. 2018;36(8):773–9.
37. Samstein RM, Lee CH, Shoushtari AN, Hellmann MD, Shen R, Janjigian YY, et al. Tumor mutational load predicts survival after immunotherapy across multiple cancer types. Nat Genet. 2019;51(2):202–6.
38. Tumeh PC, Harview CL, Yearley JH, Shintaku IP, Taylor EJ, Robert L, et al. PD-1 blockade induces responses by inhibiting adaptive immune resistance. Nature. 2014;515(7528):568–71.
39. Fehrenbacher L, Spira A, Ballinger M, Kowanetz M, Vansteenkiste J, Mazieres J, et al. Atezolizumab versus Docetaxel for patients with previously treated non-small-cell lung cancer (POPLAR): a multicentre, open-label, phase 2 randomised controlled trial. Lancet. 2016;387(10030):1837–46.
40. Maloy G, Anurag T, Ashvini Kumar D, Sanghamitra B, Yogendra M, Shalini K, et al. 719 phase 1 clinical trial design of ZM008, a first-in-class anti LLT1 antibody is a promising therapy for multiple solid cancers. J Immunother Cancer. 2023;11(Suppl 1):A814.
41. Ghosh M, Rodrigues KI, Maity S, Bhattacharjee S, Manjunath Y, Chakrabarty SP, et al. Novel monoclonal antibody therapeutics for metastatic castration resistant prostate cancer. J Clin Oncol. 2019;37(15suppl):e14222-e.
42. Maloy G, Anurag T, Ashvini D, Sanghamitra B, Yogendra M, Shalini K, et al. 1391 ZM008 a first in class monoclonal anti LLT1 antibody demonstrated clinical potential in multiple solid cancers. J Immunother Cancer. 2022;10(Suppl 2):A1445.
43. Goldman MJ, Craft B, Hastie M, Repecka K, McDade F, Kamath A, et al. Visualizing and interpreting cancer genomics data via the Xena platform. Nat Biotechnol. 2020;38(6):675–8.
44. Wickham H. Data Analysis. In: Wickham H, editor. ggplot2: elegant graphics for data analysis. Cham: Springer International Publishing; 2016. pp. 189–201.
45. Larmarange J. ggstats: Extension to'ggplot2'for Plotting Stats. 2023. R package version 0.2.1.
46. R Core Team. (2023) R: a language and environment for statistical computing, Vienna. https://www.R-project.org/
47. Davidson-Pilon C. Lifelines: survival analysis in Python. J Open Source Softw. 2019;4:1317.
48. Borgan Ø. Modeling Survival Data: Extending the Cox Model. Terry M. Therneau and Patricia M. Grambsch, Springer-Verlag, New York, 2000. No. of pages: xiii + 350. Price: \$69.95. ISBN 0-387-98784-3. Stat Med. 2001;20(13):2053–4.
49. Therneau T. A package for survival analysis in R (R package version 3.5-0). New York, NY, USA: Springer; 2023.
50. Liberzon A, Birger C, Thorvaldsdottir H, Ghandi M, Mesirov JP, Tamayo P. The Molecular signatures database (MSigDB) hallmark gene set collection. Cell Syst. 2015;1(6):417–25.
51. Boris M, Maria T, Vincent C, Mathieu A. PyDESeq2: a python package for bulk RNA-seq differential expression analysis. bioRxiv. 2022:2022.12.14.520412.
52. Love MI, Huber W, Anders S. Moderated estimation of Fold change and dispersion for RNA-seq data with DESeq2. Genome Biol. 2014;15(12):550.
53. Fang Z, Liu X, Peltz G. GSEApy: a comprehensive package for performing gene set enrichment analysis in Python. Bioinformatics. 2023;39(1):btac757.
54. Newman AM, Liu CL, Green MR, Gentles AJ, Feng W, Xu Y, et al. Robust enumeration of cell subsets from tissue expression profiles. Nat Methods. 2015;12(5):453–7.
55. Li T, Fu J, Zeng Z, Cohen D, Li J, Chen Q, et al. TIMER2.0 for analysis of tumor-infiltrating immune cells. Nucleic Acids Res. 2020;48(W1):W509–14.
56. Pedregosa F, Varoquaux G, Gramfort A, Michel V, Thirion B, Grisel O, et al. Scikit-learn: machine learning in Python. J Mach Learn Res. 2011;12(null):2825–30.
57. Ashburner M, Ball CA, Blake JA, Botstein D, Butler H, Cherry JM, et al. Gene ontology: tool for the unification of biology. The Gene Ontology Consortium. Nat Genet. 2000;25(1):25–9.
58. Yu G, Wang LG, Han Y, He QY. clusterProfiler: an R package for comparing biological themes among gene clusters. OMICS. 2012;16(5):284–7.
59. Wu T, Hu E, Xu S, Chen M, Guo P, Dai Z, et al. clusterProfiler 4.0: a universal enrichment tool for interpreting omics data. Innov (Camb). 2021;2(3):100141.
60. Colaprico A, Silva TC, Olsen C, Garofano L, Cava C, Garolini D, et al. TCGAbiolinks: an R/Bioconductor package for integrative analysis of TCGA data. Nucleic Acids Res. 2016;44(8):e71.
61. Silva TC, Colaprico A, Olsen C, D'Angelo F, Bontempi G, Ceccarelli M, et al. TCGA Workflow: analyze cancer genomics and epigenomics data using Bioconductor packages. F1000Res. 2016;5:1542.
62. Mounir M, Lucchetta M, Silva TC, Olsen C, Bontempi G, Chen X, et al. New functionalities in the TCGAbiolinks package for the study and integration of cancer data from GDC and GTEx. PLoS Comput Biol. 2019;15(3):e1006701.
63. Mayakonda A, Lin DC, Assenov Y, Plass C, Koeffler HP. Maftools: efficient and comprehensive analysis of somatic variants in cancer. Genome Res. 2018;28(11):1747–56.
64. Carey V. BiocOncoTK: Bioconductor components for general cancer genomics. 2018. R package version 1.1.16.2018.
65. Eddy JA, Thorsson V, Lamb AE, Gibbs DL, Heimann C, Yu JX, et al. CRI iAtlas: an interactive portal for immuno-oncology research. F1000Res. 2020;9:1028.

Publisher's Note